Proceedings of the First European Conference on Space Debris, Darmstadt, Germany, 5-7 April 1993 (ESA SD-01)

DIRECT METHOD FOR THE ANALYSIS OF COLLISION PROBABILITY OF ARTIFICIAL SPACE OBJECTS IN LEO: TECHNIQUES,RESULTS AND APPLICATIONS

Zakhari N.Khutorovsky,Vladimir F.Boikov,Sergey Yu.Kamensky
"Vympel" Corporation,Moscow,Russia

Abstract

The most natural "direct" method is suggested for the study of orbital missions safety and for possible collisions warning. The primary database for this approach are continuously improved estimations of element sets and other parameters for satellites in LEO.By numerical integration (with small steps) of the differential equations of motion for all objects in the database, the closest points of approach and respective time intervals for all possible pairs of objects are obtained. Simultaneously, characteristics of the geometry of possible collisions and collision probabilities are calculated. The relationship between collision probability for two dangerously approaching satellites and their geometry characteristics, coordinate errorsand parameters of relative motion is established. The basic ideas of a computer code capable of determination all close approaches are described. Results, obtained for real database in the course of half a year are discussed.

1 Introduction

Orbital flight safety evaluation for periods, ranging from few days to several years, is a necessary part of the spacecraft and orbital missions design. The hazard to space vehicle is posed by a great amount of debris, produced by more than 3000 launches and more than 100 breakups, which took place during last 35 years. It is important to be able to evaluate collision probabilities for a certain object or for chosen group of them, taking into consideration different factors.Mission duration, orbital parameters, characteristics of size and motion of the spacecraft, limiting size of debris, taken into account, geometry of conjunction event, uncertainties in initial values can be named as such factors. It is necessary to have complete data, concerning spatial distribution of satellites and characteristics of their relative motion, with special attention to the major risk regions. The list of problems can be continued, but it must be noted, that the most valuable evaluations of debris hazard are those relied on real observations and satellites catalog.

Substantial efforts were extended to fulfill those tasks during last 15 years. First of all, a number of methods, revised in Ref.1 should be mentioned. These methods relies upon space and time averaged distributions of satellites, described by spatial density. Having some specific features, they are based on general approach, developed by D.Kessler (Ref.2). The shortcomings of this approach are difficulties in consideration specific characteristics of a certain object and the difference between the real and the averaged distribution of satellites. These limitations can result in too rough evaluations, especially in collision risk analysis for individual objects.

Some recent articles deals with attempts to avoid spatial averaging. The initial database for such methods contains a set of satellites with determined orbits. D.Kessler's method is also feasible in this case, but the calculations become unwieldy. D.Rex and P.Euhler (Ref.3) suggest a semi-deterministic method, based on analytic determination of collision probability for an arbitrary pair of objects within a given time interval, using their element sets and sizes. We can't objectively judge this method, since we didn't manage to find a detailed description, but our understanding is that the formulae for collision probabilities are a time-averaged conclusion. That's why this method can't produce a real time-dependent pattern of collisions and can result in bias of relative motion parameters distributions.

The work of D.Veder and D.Tabor (Ref.4) should also be mentioned.It presents a specific method for collision probability calculations, based on the study of minimal distance (between the target satellite and the others) distribution, using the technique of asymptotic theory for extreme of order statistics. The main assumption is the random distribution of mean anomalies for all satellites at an arbitrary moment. This assumption permits to use Monte-Carlo modeling for calculations of collision probabilities. But it is not still clear enough, how does the difference between the real combination of mean anomalies and the randomly distributed one influence the final results. The article Ref.4 does not treat this issue.

We consider, that the limitations of existing methods can be eliminated only using an approach, that can be called "direct". Such approach, being the most natural, seems to avoid information losses. The primary database for this approach are continuously improved estimations of element sets and other parameters for satellites in LEO. By numerical integration (with small steps) of the differential equations of motion for all objects in the database, the closest points of approach (c.p.a.) and respective time intervals for all possible pairs of objects are obtained. Simultaneously, characteristics of the geometry of possible collisions and collision probabilities are calculated. Such approach gives natural solution for many issues of orbital missions safety evaluation, provided that the process of the search of c.p.a. is long enough, and all the necessary intermediate information is stored.

A distinguished feature of the direct method is that it provides characteristics of real conjunctions, since the primary database is real. Thus it can be used not only in design analysis, but for warning of possible real collisions in the future as well. This warning can help to take measures for updating the possibilities of collisions and for their avoidance, or to organize observations of the collision process and its consequences.

Though the physical foundations of this approach are quite reliable, the difficulties in its realization are obvious. The great amount of necessary calculations seem to make realization impossible. But we can stay, that it is not so. The problems of computer realization can be solved. We intend to demonstrate appropriate tech-

niques in this paper, composed of three main parts. The first part, treating theoretical issues, results in the basic relationship for calculation of collision probability, regarding two approaching satellites. The second part describes the basic concepts of software techniques, allowing to fulfill necessary calculations with potentially high accuracy within reasonable CPU-time. The third part presents results, obtained by this method on a real database in the course of half a year. In particular, spatial distributions of satellites and the points of possible collisions, relative motion characteristics distributions, estimations of collision probabilities for certain objects and their different subsets, maximum risk regions, possibilities of consideration non-tracked objects and future launches, are analyzed. Finally, a comparative analysis of certain results, obtained by direct method and the method of D.Kessler, is presented.

2 Basic relationship

Regarding orbital motion of many satellites, a conjunction of two, three or more objects is possible. Estimations demonstrate, that the probability of collision of more than two satellites is negligible. Thus it is considered, that the collision may occur only between two approaching satellites. The problem of collision probability determination is reduced to easier task for two objects regarding a given time interval. Other probabilities can be obtained by summing up for all possible satellite pairs and needed time intervals.

Let the distributions of motion parameters for centers of both objects in rectangular coordinate system $p_1(r_1, v_1, t_1); p_2(r_2, v_2, t_2)$ be determined for arbitrary moment t. Here $r_1 = (x_1, y_1, z_1); r_2 = (x_2, y_2, z_2); v_1 = (\dot{x}_1, \dot{y}_1, \dot{z}_1); v_2 = (\dot{x}_2, \dot{y}_2, \dot{z}_2)$ are position and velocity vectors.

Then the collision probability for two objects at the moment t can be expressed by a formula

$$P_t(C) = \int_{\Omega(t)} p_1(r_1, v_1, t_1) p_2(r_2, v_2, t_2) dr_1 dr_2 dv_1 dv_2 \tag{1}$$

and $\Omega(t)$ is the region, where collision occurs. This region can be represented as follows. Suppose the position of the first object is fixed. The boundary of the region is produced by the center of the second object, regarding sliding of the second object by the surface of the first one . So, the initial situation is equivalent to collision of the first object (target), considered to occupy the region $\Omega(t)$, with the second one (projectile),taken as a point mass. The size of the target does vary, depending on different relative positions of approaching objects . If both objects are spheres with diameters d_1 and d_2 , the target will be $(d_1 + d_2)$ - diameter sphere, independent of the relative position. Further the first object will be considered a target $\Omega(t)$ and the second one - a point mass.

Collision probability calculations suppose integration of Eq.1 over all possible moments. But there's no need to do that. It is sufficient to integrate only over the moments, satisfying $|r_1 - r_2| < \delta r_1 + \delta r_2 + d_{max}$, where δr_1 and δr_2 are maximum errors in position determination for each satellite, d_{max} - maximum size of the target. These moments form a certain interval. We shall call it the interval of dangerous approach T_a . The points outside T_a are of no interest because the collision probability for them equals zero. The data, presented at Fig.1, 3 and 15 demonstrate, that the average length of this interval is approximately 5s. All further considerations will deal with the moments within T_a .

We consider the following assumptions to be true :

1.The relative motion is in straight lines. $r_2(t) - r_1(t) = r_2 - r_1 + \Delta v(t - t_0)$, where $\Delta v = (\Delta\dot{x}, \Delta\dot{y}, \Delta\dot{z})$ - is a constant vector, t_0 - a fixed moment inside T_a .

2.The velocities $v_1(t)$ and $v_2(t)$ are determined precisely (i.e. the errors of their determination equal 0).

3.The uncertainties in position of the second object (projectile) greatly exceeds the size of the target, that means p_2 is constant within the target $\Omega(t)$.

These assumptions does not lead to substantial limitations. Assumption 1 is valid, because simple estimations can prove, that within interval of 20 s, symmetrical about the c.p.a.,the relative motion trajectory deviates from straight line less than 0.05 km. This deviation can be neglected, since minimum coordinate errors are much greater (Fig.1). Assumption 2 is true, since the errors in velocity determination usually don't exceed 1 m/s and can be neglected within the interval of dangerous approach T_a . Finally, assumption 3 is valid because the sizes of largest satellites are an order of magnitude smaller, than the values of minimum mean-square errors in position determination.

We proceed to the derivation of the main formula. Suppose, parameters of the center of target r_1, v_1 are determined. Then for the interval $(t, t + \Delta t)$ the surface of the target $\Omega(t)$ can be crossed by the point, distant not more than $(v_2 - v_1)n^T \Delta t$, where n is normal to the target surface and n^T means transposed vector. Probability of this event is conventional probability of collision of two objects within the interval $(t, t + \Delta t)$, by convention that the center of the target is r_1, v_1 . It is equal to

$$\Delta P_t(C|r_1, v_1) = \Delta t \int_{\Omega(t)} (v_2 - v_1) n^T p_2(r_2, v_2, t) dS \tag{2}$$

and integration is over the surface of $\Omega(t)$.

Under the assumptions 2 and 3

$$\Delta P_t(C|r_1, v_1) = \Delta P_t(C|r_1) \approx \Delta t |\Delta v| S(t) p_2(r_2(r_1)) \tag{3}$$

where $S(t)$ is the area of $\Omega(t)$, projected to the plane, normal to Δv (collision cross-section), $r_2(r_1)$- the value of r_2 in the center of the target.

Collision occurs when $r_2(t) - r_1(t) = 0$. Thus, according to assumption 1, $r_2 - r_1 + \Delta v(t - t_0) = 0$, and

$$r_2(r_1) = r_1 - \Delta v(t - t_0) = r_1 - \Delta v\tau(\tau = t - t_0) \tag{4}$$

Unconditional collision probability for the interval $(t, t + \Delta t)$ is equal to

$$\Delta P_t(C) = \int \Delta P_t(C|r_1) p_1(r_1) dr_1 \tag{5}$$

To determine Eq.5, suppose that for the moment t_0 , position vectors for the satellites have normal distributions, characterized by $\hat{r}_1, K_1, \hat{r}_2, K_2$ respectively, i.e.

$$p_i(r_i) = (2\pi)^{-1.5} det K_i^{-0.5} \exp(-0.5(r_i - \hat{r}_i) K_i^{-1} (r_i - \hat{r}_i)^T), \; i = 1, 2 \tag{6}$$

where $\hat{r}_1, \hat{r}_2$ are predicted to the moment t_0 positions of objects; K_1, K_2 - correlation matrices of position determination errors at the moment t_0; $detK_1, detK_2$ - determinants; K_1^{-1}, K_2^{-1} - reverse matrices.

Substituting Eq.3,4,6 into Eq.5, we have

$$\Delta P_t(C) = k_1 \int \exp(-0.5((r_1 - \hat{r}_2 - \Delta v\tau)K_2^{-1}(r_1 -$$

$$- \hat{r}_2 - \Delta v\tau)^T + (r_1 - \hat{r}_1)K_1^{-1}(r_1 - \hat{r}_1)^T))dr_1 \quad (7)$$

where $k_1 = \Delta t S(t)|\Delta v|(2\pi)^{-3} detK_1{}^{-0.5} detK_2{}^{-0.5}$. Performing obvious, though bulky, calculations, we obtain

$$\Delta P_t(C) = k_2 \exp(-0.5(\Delta\hat{r}+\Delta v\tau)(K_1+K_2)^{-1}(\Delta\hat{r}+\Delta v\tau)^T) \quad (8)$$

where

$$k_2 = \Delta t S(t)|\Delta v|(2\pi)^{-1.5}(detK_1 detK_2 det(K_1^{-1}+$$

$$K_2^{-1}))^{-0.5}; \Delta\hat{r} = \hat{r}_2 - \hat{r}_1$$

The total collision probability in the course of considered dangerous approach equals

$$P(C) = \int \frac{\Delta P_t(C)}{\Delta t} dt \quad (9)$$

integrating over interval T_a .

Similar calculations result in

$$P(C) = k_3 \exp(-0.5(k_{rr} - k_{rv}^2 k_{vv}^{-1})) \quad (10)$$

where

$$k_3 = \tilde{S}|\Delta v|(4\pi^2 detK_1 detK_2 det(K_1^{-1} + K_2^{-1})k_{vv})^{-0.5};$$

$$k_{rr} = \Delta\hat{r}(K_1 + K_2)^{-1}\Delta\hat{r}^T;$$

$$k_{vv} = \Delta\hat{v}(K_1 + K_2)^{-1}\Delta\hat{v}^T;$$

$$k_{rv} = \Delta\hat{r}(K_1 + K_2)^{-1}\Delta\hat{v}^T;$$

This is the final formula for probability of collision of two objects in the region of their dangerous approach. Let us discuss this result.

Eq.10 reads that collision probability depends on : relative velocity $|\Delta v|$, collision cross-section $\tilde{S}$ (taken for a certain moment $\tilde{t}$ within the interval of dangerous approach), correlation matrices of position determination errors K_1 and K_2 , predicted to the moment t_0 positions of both objects $\hat{r}_1$ and $\hat{r}_2$. There is no real dependence on the moment t_0 , since we can easily reveal, that under assumption 1, $P_{t_0}(C) = P_{t_1}(C)$, where t_1 is an arbitrary moment within the dangerous approach interval. It is feasible to use as t_0 the moment of the minimum distance,or the moment, providing $k_{rv} = 0$. A certain intermediate value, depending on the approach considered, must be assigned to $\tilde{S}$. No problems exist for spherical forms, because S(t)=const.

It will be instructive to consider an example. Supposing the position uncertainties for both objects are the same in all directions and have root-mean-square deviations σ_1 and σ_2 respectively. Using Eq.10, we obtain

$$P(C) = \frac{S}{2\pi(\sigma_1^2 + \sigma_2^2)} \exp(-\frac{\Delta r_{min}^2}{2(\sigma_1^2 + \sigma_2^2)}) \leq \frac{S}{2\pi(\sigma_1^2 + \sigma_2^2)} \quad (11)$$

where Δr_{min} is the minimum distance between two satellites.

The right side of Eq.11 represents the ratio of collision cross-section and the doubled area of the position errors ellipse. Finally, it must be mentioned, that assumption 2, and especially 3,are not valid in certain situations.It is possible to obtain formulae for P(C) regarding such cases, but their design will be much more sophisticated.

3 Computations procedure

The search for dangerous approaches for n_t tracked satellites is carried on within a time interval (t_{in}, t_f). For all satellites element sets E and correlation matrices of errors K_E are supposed to be determined for certain moments, earlier than t_{in} . Procedure for calculation of approaches characteristics is as follows. Taking small steps $h(h \ll t_f - t_{in})$ from t_{in} up to t_f, propagation of parameters for all satellites to the moments $t_i = t_{in} + ih(i = 0, 1, 2...)$ is fulfilled. The search for approaching within the interval $(t_i, t_i + h)$ pairs is carried out. For all such pairs geometry characteristics of conjunctions and collision probabilities are calculated. The idea of algorithm is obvious. The main problem to be solved is to carry out calculations within reasonable CPU-time. In fact, taking $t_f - t_{in} = 1$ day, $h = 50s, n_t \approx 10^4$, it is necessary to perform $\approx 10^7$ propagations and run down $\approx 10^{11}$ pairs of satellites. Taking no special measures for computations arrangement, it is impossible to fulfill calculations within tolerable CPU-time (regarding a $10^6 \div 10^7$ operations per second computer). Parameters propagation and search for approaching pairs are the main parts of the procedure. They need a more detailed consideration.

3.1 Propagation algorith

The basic algorithm is described in Ref.5,6. Propagation is carried out considering mean element sets $E = (\lambda, L, \theta, \Omega, h, k); \lambda = M + \omega; L = \sqrt{\mu a}; \theta = \cos i; h = e\sin\omega; k = e\cos\omega$; where $M, \omega, a, i, e, \Omega$ are the mean anomaly, argument of perigee, semi major axis, inclination, eccentricity, right ascension of ascending node respectively; μ - gravitational constant. Earth oblateness, expressed by zonal and tesseral harmonics (included up to eight order) and atmosphere, presented by dynamic model, are taken into account. For extrapolation interval not exceeding three days, real prediction errors are in the average $\approx 0.1km$ for radial and lateral directions , and $\approx 0.2km$ adding 10% of the atmospheric drag for forward direction (Ref.7).

The algorithm consumes $10^3 \div 10^4$ operations per single reference depending on the handling mode (Ref.7). Authors are unaware of more rapid procedures, providing the same accuracy. But even these cha- racteristics cannot meet our requirements.They must be reduced by an order of magnitude or more. And the necessary conditions still remain the correct determination of all conjunctions

and the estimation of their characteristics with methodical errors, not exceeding errors of the basic propagation algorithm.

Reasonable CPU-time without losses in the efficiency, can be obtained, introducing a three stage prediction procedure. This procedure implies that basic algorithm is used, if necessary, only at the last (third) stage. For other stages, much simpler prediction methods, ensuring enough accuracy to select the pairs, impossible to collide within the interval $(t_i, t_i + h)$, are applied.

Procedure of second order polynomial fit extrapolation in rectangular coordinate system x,y,z is used for the first stage. More comprehensive and more accurate procedure of the second stage specifies the coefficients of polynomial fit within $\tau_p (\tau_p \gg h)$. The second stage procedure is a polynomial extrapolation of mean element sets E, followed by calculations of $x, y, z, \dot{x}, \dot{y}, \dot{z}$ by general Keplerian formulae (Ref.8). Polynomial fit of orders $s_\lambda, s_L, s_\theta, s_\Omega, s_e, s_\omega$ is fulfilled regarding parameters $\lambda, L, \theta, \Omega, e, \omega$ respectively. These polynoms approximate variations of elements E inside the interval (t_{in}, t_f). Their coefficients are calculated by the least squares method, applied to s evenly spaced inside the interval (t_{in}, t_f) values of the elements, obtained by the basic prediction algorithm $(s \geq max(s_\lambda, s_L, s_\theta, s_\Omega, s_e, s_\omega))$. The sequence of applying different prediction algorithms is ruled by the procedure, employed to the search of close approaches. We proceed to its description.

3.2 Search for approaching pairs procedure

Algorithm is composed of two parts: preliminary selection and refinement. Preliminary selection, using the simplest first stage prediction,reveals pairs of satellites, possible to collide within the interval $(t_i, t_i + h)$. It is followed by stepwise refinement. Not more than three steps are made, provided each step implies a more comprehensive prediction procedure. If the third step results in a decision, that collision may occur, its probability and geometry characteristics are calculated.

3.2.1 Algorithm for primary selection

Algorithm for primary selection of dangerously approaching pairs is intended to fulfill the following task. Let the positions $x_q, y_q, z_q; q = 1, 2...n_t$ of all satellites be determined for fixed moment. We are to find pairs of j and k, which satisfies the condition $(x_j - x_k)^2 + (y_j - y_k)^2 + (z_j - z_k)^2 < c^2$, where c is a threshold, chosen to satisfy two contradictory conditions.On one hand, it must provide the efficiency of preliminary selection, i.e. substantially reduce the number of pairs, subjected to consequent analysis. On the other hand, no misses of dangerous approaches within interval $(t_i, t_i + h)$ should take place. If the determination of element sets is sufficiently accurate, the threshold value c is defined only by the step of the motion equations integration h.

This is the most tedious part of the procedure. Having $t_f - t_{in} = 1$ day and $h = 50s$, we are to perform primary selection of $\approx 10^{11}$ pairs of satellites, and direct realization of the procedure consumes $\approx 10^{12}$ operations. To meet the requirements for CPU-time, this value is to be reduced by a factor of $10^2 \div 10^3$. The required reduction can be obtained by employing the following technique of computer coding, intended to make use of the specific features of the computer.

Representing coordinates x, y, z of a satellite as integer values $m = E(x/c), n = E(y/c), p = E(z/c)$ ($E(*)$ denotes the integer part), we are to search objects, approaching the satellite, indexed q, only among those, which have the difference between m, n, p and m_q, n_q, p_q respectively, equal to 0 or ± 1.
For computer realization this algorithm can be formalized as follows. We introduce binary scales $X_\alpha = (X_{\alpha_1}, X_{\alpha_2}, \ldots, X_{\alpha_{n_t}}), Y_\beta = (Y_{\beta_1}, Y_{\beta_2}, \ldots, Y_{\beta_{n_t}}), Z_\gamma = (Z_{\gamma_1}, Z_{\gamma_2}, \ldots, Z_{\gamma_{n_t}})$, of length n_t, where α, β, γ range the same values, as m, n, p. X_α scale (or Y_β, Z_γ respectively) indicates the objects, having the value of m (n or p respectively) equal to $\alpha - 1$,or α,or $\alpha + 1 (\beta - 1, \beta, \beta + 1; \gamma - 1, \gamma, \gamma + 1$ respectively). For a given satellite, indexed q, the indexes of approaching objects will correspond to the units of the scale $V_q = X_{m_q} \bigcap Y_{n_q} \bigcap Z_{p_q}$.

This procedure is realized in the form of two cycles, running through all objects. The first cycle is intended to calculate parameters m, n, p for all objects, and to produce all the scales $X_\alpha, Y_\beta, Z_\gamma$ putting units in appropriate places. The second, most tedious cycle, defines V_q scale and the desired pairs.

Advantages in CPU-time, provided by the described preliminary selection procedure, have their origin in the existence of rapid commands, executing operations with binary scales. For example, regarding a computer, processing 64-position words, this technique can reduce CPU-time by a factor of $40 (c = 400km)$. If the computer is capable of performing block logical operations, the gain would increase.

3.2.2 The refinement algorithm

The refinement algorithm is aimed to find a moment t_{min} , corresponding to the minimum distance between two objects within $(t_i, t_i + h)$. For the first step prediction of the first stage is used. If the obtained minimum distance is less than $c_1 (c_1 < c)$, we proceed to the second step.Prediction of the second stage is used.If the minimum distance is less than $c_2 (c_2 < c_1 < c)$, we proceed to the third step. For the third step the basic prediction procedure is used. If the obtained minimum distance is less than $c_3 (c_3 < c_2 < c_1 < c)$, proceed to collision probability calculations, according to the formulae of the previous section. For each step straight-line approximation of relative motion in the vicinity of t_{min} is used.This allows to calculate t_{min} according to simple formula for extreme of square function.

4 Results

4.1 Primary database

The described procedure was applied to evaluate close approaches characteristics for satellites in LEO (perigee altitude less than 4000 km). Russian Space Surveillance System maintains the catalog of these objects. Their parameters are continuously updated in real time scale.This process is described in Refs. 7,9, as well as the main characteristics of catalog. Here we should mention only those, important for further considerations.

Fig.1 presents the distribution of satellites (distribution step 0.1 km) according to root-mean-square deviations of errors, considering orbital coordinate system: σ_r - in radial direction, σ_s - in lateral (binormal) direction, σ_v - in the direction of motion (transversal). Considering s and r directions,the distributions correspond to the moment t_u of the last updating, coincident with the moment of the last observation. The value of t_u varies for different satellites and does not exceed the current moment t. Distribution of satellites according to $t-t_u$ with step 0.1 day is presented by Fig.2. Considering parameter v, the distributions are presented: for the moment of the last updating (σ_v), for the current moment (σ_{vt}), and regarding prediction for k days from the current moment (σ_{vtk}). As evident from Fig.1,2, for 50% of tracked objects: $t - t_u < 0.6$ days, $\sigma_r < 0.35km, \sigma_s < 0.35km, \sigma_v < 1.6km, \sigma_{vt} < 2.0km, \sigma_{vt1} < 3.1km, \sigma_{vt2} < 5.1km, \sigma_{vt3} < 7.6km, \sigma_{vt5} < 14km, \sigma_{vt7} < 24km, \sigma_{vt10} < 43km$, and about 18% of objects have for the current moment $\sigma_{vt} > 50km$.

Fig.3 shows the distribution of satellites according to mean size, obtained from radar cross-section ($70cm$ wavelength signal). For the object of arbitrary configuration we consider the mean size d (or size, for further considerations) to be the diameter of a circle, with the area, equal to the average of projected areas S regarding all possible projections to the normal plane. One notes, from Fig.3, that the mean value for d is $1.1m$, minimum $0.1m$, maximum $10m$. For 50% of satellites $d < 0.7m$. Averaged over all tracked satellites $\overline{S}$, mean projected area S is equal to $2.1m^2$.

4.2 Choosing algorithm parameters

The accuracy of orbital parameters decline with increase of propagation interval. Thus, the calculations interval (t_{in}, t_f) is desirable to be close to the current moment t and not too extensive. On the other hand, evaluation of certain characteristics of dangerous approaches requires long intervals, and, considering operational practices, in particular, collision warning, it is necessary to have $t_{in} > t$.

Regarding these requirements, the following mode to execute the procedure is chosen: everyday calculations on the current database, with propagation to the nearest day.Calculations revealed the step $h = 50s$ to provide reasonable CPU-time. It corresponds to the preliminary selection threshold $c = 400km$. The interval τ_p for polynomial approximation of objects motion in rectangular coordinate system is chosen equal to $500s$, and the order of polynoms, approximating time dependence of the elements are $s_\lambda = 4, s_L = 3, s_\theta = 0, s_\Omega = 2, s_e = 3, s_\omega = 2$ respectively. Threshold values c_1, c_2, c_3 depend on the errors of determination and propagation of orbits. Analytic estimations and calculation runs (not to be considered here) revealed the values of $c_1 = 90km, c_2 = 40km, c_3 = 30km$.

If the errors of the element set for the satellite are great enough, confident determination of the conjunction event becomes impossible. But such object still produce a certain contribution to cumulative collision probability. To take proper account of these contributions, the root-mean-square deviations of errors at the moment of approach had the upper limits of $5km$ for radial and lateral directions, and $10km$ for transversal direction.

Since July 1992, everyday calculations in the previously described mode, are organized. Necessary information, subjected to further analysis, is stored in the archives of dangerous approaches (ADA). The approach is considered to be "dangerous",in the case of either the distance between satellites is less than $3km$, or the distance is less than $30km$ and and the probability of collision exceeds 10^{-11}. About 2000 dangerous approaches are revealed daily. For each dangerous approach the following characteristics are stored in ADA: international designator, type, responsible country, size, element set, accuracy characteristics (for each satellite), geometry characteristics of relative motion and collision probability (50 parameters in the total). Results of analysis, carried out for ADA, stored for half a year, are discussed further.

4.3 Spatial parameters distributions

Satellites spatial density is usually obtained by means of analytical technique,developed by D.Kessler (Ref.2), under the assumption of Keplerian motion. Stepwise numerical integration of differential equations provide the real spatial distribution, free of any limiting assumptions. This distribution can be conveniently presented in spherical coordinate system r, φ, λ (r-distance,φ-latitude,λ-longitude).

Fig.4,5 depicts distribution of satellites, according to altitude h and latitude $\varphi - f_h, f_\varphi$, with distributions steps $\Delta h = 10km$ and $\Delta\varphi = 1°$ respectively. Collision probabilities distributions (with the same distribution steps) p_h, p_φ are presented in the same plots. The values $f_h(h)$ and $f_\varphi(\varphi)$ indicates the fractions of satellites, resident within the intervals $(h-\Delta h, h)$ and $(\varphi-\Delta\varphi, \varphi)$ respectively, among all the objects with $h < 3000km$. The values $p_h(h)$ and $p_\varphi(\varphi)$ indicates the probability of collision of two satellites within intervals $(h-\Delta h, h), (\varphi-\Delta\varphi, \varphi)$, provided that collision occurs in $h < 3000km$.

Figures 6-9 show altitude-latitude distributions of satellites $f_{h,\varphi}$; collision probabilities $p_{h,\varphi}$, and their topographic projections to the plane (h, φ).Distributions steps are $\Delta h = 50km, \Delta\varphi = 3°$. Figures 10,11 illustrates mean satellite's size as function of altitude $\overline{d}(h)$ and latitude $\overline{d}(\varphi)$, obtained while integrating differential equations for tracked objects. The analysis of fig.4-11 allows to note the following.

1.Altitude distributions of satellites and their collision probabilities present two major maxima at $800-1000km$ and $1500km$, with events frequencies for a $10km$ band $0.01 \div 0.04$. The minimum, corresponding to $h = 1200 \div 1300km$ lies between them. For satellites distribution the frequency of falling into the same intervals within this region is 0.0025, and for collision probabilities distributions - 0.0002.

2.Latitude distribution of satellites is near to uniform, declining at $|\varphi| > 63°$ and certain increase at $|\varphi| < 8°$. Increase at $|\varphi| < 8°$ region is apparently caused by ≈ 200 satellites, having inclinations $i < 8°$. Small local maxima corresponds to the most populated inclinations of $7°, 28°, 65°, 74°, 81°$. Latitude distribution of the points of closest approaches within the region $|\varphi| < 60°$ is nearly uniform, with average event frequency 0.0035 (for a $1°$ -width layer),but outside this region the distribution has three evident maxima, corresponding to inclinations peaks $81°, 74°, 65°$, where the event frequency exceeds the average by a factor of $4-6$.

3.Distribution of satellites and their collision probabilities in general correspond each other, taking into account the quadratic dependence of collision probability within a certain region, on the average number and mean size of objects,resident in the region.

4.Altitude-latitude distribution of satellites has two nearly equal maxima ≈ 0.0025, corresponding to $h = 1450 - 1500km, \varphi = \pm(72° - 75°)$ and $h = 900 - 1000km, \varphi = \pm(63° - 66°)$ in both semi-spheres, and a slightly lower maximum ≈ 0.0015 in $h = 950 - 1000km, \varphi = \pm(78° - 84°)$. The first two maxima are produced by nearly circular orbits $h = 1500km, i = 74°$ and $h = 900 - 1000km, i = 65°$; the third one - by the orbits with $h = 900 - 1000km, i = 81°$.

5.Altitude-latitude distribution of collision probability is not quiet symmetrical in latitude.That is caused by the influence of the most dangerous individual conjunctions.The greatest maximum 0.019 is placed in $h = 880km$ and $\varphi = -61°$, where the most dangerous approach occurred on 26.08.92 (Appendix 1). The consequent maximums are 0.016 and 0.013 for $h \approx 950 - 1050km$ and $\varphi = \pm(81° - 84°)$. They correspond to orbits with maximum collision risk (Fig.19-21). Slightly lower are the maximums 0.0085 and 0.0087, caused by orbits with $h \approx 1450 - 1500km, i = 74°$. The peaks of 0.005 and 0.007 are present at altitudes $950 - 1000km$ and latitudes $\pm(63° - 66°)$. Individual non-symmetrical peaks, for example $h = 850km, \varphi = -(33° - 36°); h = 800km, \varphi = -(6° - 9°); h = 1000km, \varphi = (48° - 51°)$ correspond to major conjunctions, occurred on 15.11.92, 08.08.92 and 27.12.92.(Appendix 1).

6.Comparison of altitude-latitude distributions of satellites and collision probabilities is inconvenient due to the influence of major conjunctions, producing non-symmetrical in φ maxima. Without taking them into consideration, one can see a following picture. The first three maxima of both distributions are the same. But the sequence of their magnitudes does differ. The first and the third peaks of the satellites distribution correspond respectively to the second and the first peaks of collision probability distribution. One of them corresponds to the region $h = 1450 - 1500km, \varphi = \pm(72° - 75°)$, the other - to $h = 950 - 1000km, \varphi = \pm(81° - 84°)$. The amount of objects , present in the first region, is 1.7 times greater,than for the second one. But the collision probability for the second region is 1.7 times greater. One can explain this effect, noting that much larger satellites are resident in the second region (Fig.11).

7.Mean satellite sizes range from $0.8m$ to $1.5m$, depending on latitude, and $0.6m$ to $3.7m$ depending on altitude. The region of least mean sizes corresponds to $h \approx 1040 - 1080km$, and of greatest sizes-to $320 - 330km$.

4.4 Distribution of relative motion parameters

Distribution of relative motion parameters is obtained by statistical processing of computed close approaches characteristics. The Table.1 presents daily averaged number of satellite pairs $\overline{n}_p(\Delta\rho)$, approaching for a distance less than $\Delta\rho$ (regarding varied $\Delta\rho$). Distribution of amount of days (a year) in accordance with the number of satellite pairs,having approach distance less than $1km$ (for a day interval) is depicted in Fig.12.

In the course of half a year ≈ 67000 pairs of satellites approached for a distance $3km$ or less. Figures 13-17 show some relationships, based on the analysis of these pairs. Fig.13,14 depicts the mean relative velocity for two approaching satellites as a function of altitude (latitude) of the closest point of approach. Fig.15 presents distributions of the number of approaches and collision probability, according to relative velocity v_{rel} (distributions step $\Delta v_{rel} = 0.1km/s$). Fig.16,17 demonstrate distributions of the number of approaches and collision probabilities according to the azimuth α and location angle β in orbital biconical coordinate system, with the origin in center of the satellite, greater in size. Distributions steps are $\Delta\alpha = 3°, \Delta\beta = 1°$. Orbital biconical coordinate system is as follows. Origin of coordinates - the position $\vec{r}_1$ of the first satellite. The local horizontal plane pass through the origin and is normal to $\vec{r}_1$. Azimuth α - the angle between velocity vector $\vec{v}_1$ of the first satellite and vector of relative position of the second satellite $\vec{r}_2 - \vec{r}_1$. Location angle β - the angle between the local horizontal plane and $\vec{r}_2 - \vec{r}_1$. The direction of approach $\vec{r}_2 - \vec{r}_1$ in the case of long distancies ($|\vec{r}_2 - \vec{r}_1| \ll min|\vec{r}_2(t) - \vec{r}_1(t)|$) and small displacements is characterized by relative velocity vector $\vec{v}_2 - \vec{v}_1$. Analysis of data, presented in Fig.13-17 draws to the following conclusions.

1.Mean relative velocity $\overline{v}_{rel}$ has the value of $11.6km/s$, being averaged over the amount of approaches, and $12.1km/s$ averaged over collision probabilities. Medians of these distributions are $13.3km/s$ and $13.6km/s$ respectively. Distributions of relative velocity according to the number of approaches and collision probabilities are evidently asymmetrical and polymodal. The major maximum of these distributions corresponds to $v_{rel} = 14.8km/s$. The next maximum is 20% lower and corresponds to $v_{rel} = 14.4km/s$. The frequency of events within the distribution step, in the vicinity of these maxima are equal to 0.067 and 0.055 respectively.

2.Dependent of altitude and latitude, the relative velocity, averaged over the amount of approaches, ranges from $8.0km/s$ to $12.7km/s$, and averaged over collision probability, ranges from $9.9km/s$ to $13.4km/s$. The maximum values of $\overline{v}_{rel}$ relates to region $|\varphi| < 7°$ and $500km < h < 850km$. Decrease of $\overline{v}_{rel}$ with the increase of altitude and absolute value of latitude, corresponds to the mode of v_{rel} behavior for circular orbits. The peaks of the $\overline{v}_{rel}(\varphi)$ in high latitudes, apparently correspond to the most frequently used inclinations. Predomination of conjunctions with objects in high-elliptical orbits in altitude region $h < 500km$ and $h > 1700km$, results in abrupt decrease of $\overline{v}_{rel}(h)$ (averaged over amount of approaches) in these altitudes. But we can not see this effect,considering $\overline{v}_{rel}(h)$, averaged over collision probabilities. The reason is the following. The errors of position determination for a satellite in high-elliptical orbit, greatly exceeds the errors for object in a near circular orbit.Thus, the probabilities of collision with such objects and their contribution to the magnitude of respectively averaged relative velocity, is minor.

3.The approach of the second satellite occurs, as a rule, from the forward direction (regarding the motion of the first satellite), at small location angles.

4.5 Cumulative collision probabilities

Figure 18 depicts the variations of daily collision probability, concerning the whole catalog. We can see, that the daily collision probability remains permanent enough,and

deviates from its mean value,equal 0.81×10^{-4} not more than a factor of 1.5-2 (upwards or downwards), not taking into consideration individual maxima, corresponding to the most dangerous approaches (Appendix 1).

Collision probabilities for different classes of satellites were evaluated, using data, stored for half a year. Results for the most interesting subsets of satellites (adjusted to annual) are as follows: all tracked satellites - 0.0295 (100 %), launch elements - 0.0291 (98.6 %), break-up debris - 0.0105 (35.9 %), satellites with period more than 200 min - 0.000071 (0.24 %), accredited to USA - 0.0139 (46.8 %), accredited to Russia - 0.0257 (87.1 %), accredited to China - 0.00091 (3.1 %), accredited to ESA - 0.00071 (2.5 %), accredited to Japan - 0.00055 (1.9 %), accredited to France - 0.00032 (1.1 %), operational - 0.0040 (13.3 %), radiation-hazardous - 0.00093 (3.1 %), space station "Mir" - 0.000050 (0.16 %).

It is possible to evaluate collision probability for an arbitrary chosen satellite. But the results will depend on the approaches, occurred to this satellite in last half of 1992. Calculations demonstrated, that for different objects in close orbits and of similar size, cumulative collision probability may differ several times, or even an order of magnitude. But, regarding a highly-populated region, we can evaluate precisely enough the average expected probability of collision for imaginary satellite of a fixed size. It can be fulfilled by adjustment to a required size all the collision probabilities, stored for all objects in considered region, calculation of cumulative probabilities and averaging them over all satellites of the region.

Figures 19-21 presents obtained by this technique collision probabilities for imaginary object in accordance with its size and altitude of circular orbit (for three inclination regions: $65° - 75°, 75° - 85°, 95° - 105°$). Averaging for each (i, h)-region, sized $10° \times 100km$, was fulfilled, considering only satellites, tracked through the whole last half of 1992 and satisfying the conditions: $d > 0.5m$ and $e < 0.01$. Corresponding amounts of these objects are depicted in the Table 2.

Figures 19-21 show the increase of collision probability with increase of object's size. This growth is quadratic only for objects of rather big size (collision probability for a $10m$ satellite is approximately twice greater than $7m$ sized one). For smaller sizes the increase is less than quadratic, and for $d < 3 - 4m$ does not exceed linear. Collision probability for $10m$ object exceeds that for $1m$ sized, by a factor of 15-25. Regarding the inclination region $65° - 75°$ maximum collision probability corresponds to altitudes $750 - 1050km$, for $75° - 85°$ region - to altitudes $850 - 950km$, and for $95° - 105°$ region - to altitudes $550 - 650km$ and $750 - 1050km$. The greatest collision probability relates to the satellites with $i \approx 75° - 85°$ and $h = 850 - 950km$. For $d = 1m$, this probability, adjusted to annual, equals 0.27×10^{-4} . It should be noted, that this value is confident enough, being obtained by averaging of the data, concerning 62 satellites.

4.6 Maximum risk regions

It is of interest to study the most dangerous approaches and satellites of greatest collision risk for the second half of 1992. The Table 3 shows the daily number of approaches $\overline{n}_c(p_1, p_2)$ with collision probabilities inside the interval p_1, p_2 . Collision probability for most dangerous approaches exceeds 10^{-5} . During second half of 1992 140 approaches of that sort occurred. Characteristics of several of them, related with the greatest collision probabilities, are presented in Appendix 1, which contains follows columns: 1-number, 2-international designators of approaching satellites, 3-types, 4-responsible countries, 5-mean sizes (m), 6-root-mean square errors of positions determination of the moment of approach (forward direction, radial and lateral directions (km)), 7-inclinations , 8-maximum and minimum altitudes over Earth surface (km), 9-Greenwich moment of approach(day,month,year,hours,minutes,seconds), 10-minimal distance between objects (orbits) (km), 11-relative velocity of approach (km/s), 12-altitude over Earth surface corresponding to closest approach (km), 13-latitude of c.p.a.projection to Earth surface, 14-collision probability.

The most dangerous was the approach of two "Meteor-1" satellites (international designators 74-25-1 and 75-124-1) that took place on 26.08.92 at $01^h59^m31.55^s$. The calculated collision probability was 0.24×10^{-3} .

Appendix 2 contains characteristics of all approaches, occurred to space station "Mir" for the same time interval.It contains follows columns: 1-number of approach, 2-international designators of the approaching satellite, 3-type, 4-mean sizes (m), 5-inclination (degrees), 6-maximum and minimum altitudes over Earth surface (km), 7-Greenwich moment of approach(day,month,year,hours,minutes,seconds), 8-minimal distance between objects (orbits) (km), 9-relative velocity of approach (km/s), 10-altitude over Earth surface at the moment of approach (km), 11-latitude of c.p.a.projection to Earth surface (degrees), 12-angle α between the space station velocity vector and relative velocity vector (degrees), 13-angle β between the horizontal plane (with respect to space station) and relative velocity vector (degrees), 14-collision probability.

Approach to "Cosmos-1508" satellite, occurred on 08.11.92 at $10^h19^m01.20^s$ turned to be the most dangerous. The satellite approached the space station at a distance $0.3km$. with relative velocity $12.7km/s$. Collision probability was 0.21×10^{-4} .

In the course of 0.5 year ≈ 350000 approaches at distances less than $3km$, or at distances less than $30km$ with collision probabilities more than 10^{-11} were cataloged in ADA. Cumulative collision probability was evaluated for each satellite, and they were ranked by the magnitude of this probability. The result was the list of satellites, which posed the major hazard during the last half of 1992. Appendix 3 presents certain data, concerning these objects.It contains follows columns: 1-number, 2-international designator, 3-type, 4-mean size (m), 5-inclination(degrees), 6-apogee and perigee altitudes over Earth surface (km), 7-amount approaches, occurred to the satellite in the course of half a year, 8-cumulative collision probability (summed over all approaches).

Two satellites "Meteor-1" (international designators 74-25-1 and 75-124-1) were revealed as most hazardous. Collision probability for both of them is equal to 0.26×10^{-3} . Collision risk for those satellites was posed by unique dangerous approach between them, that occurred on 26.08.92. One notes, that evident correlation exists between the most hazardous satellites and the most dangerous approaches from Appendix 1. For the majority of satellites in the upper part of the list of most hazardous objects, the cumulative collision probability was determined by the single dangerous approach, from the upper

part of the list of the most dangerous approaches.

4.7 "Invisible" debris and new launches

Not all orbiting objects are tracked by Russian Space Surveillance Network now. Thus, the present catalog is not complete, and is to be enlarged in the future, due to putting into operation new sensors and modification of the old ones. The catalog will increase also because of future launches to LEO. The majority of non-tracked objects in LEO belongs to the small sized break-up debris. Consideration of non-tracked objects in collision probability calculations become possible, since their spatial and sizes distribution $f_{ut}(h, \varphi, d, t)$ is determined.In fact, probabilities of all collisions from ADA can be recalculated, considering all the untracked objects of given size, using probability theory methods. This formulas consider the spatial density of tracked break-up debris $f_t(h, \varphi, d, t)$ evaluated in the process of the search of dangerous approaches.

Proper account of the future-launched satellites is more difficult, because it is necessary to consider orbits evolution under the influence of perturbating factors (primarily, atmospheric drag and solar radiation pressure), and possible future breakups. But such account may turn to be ineffective, due to great uncertainties in the future environment. That's why, of certain interest is the account of the future launches and breakups under the assumption, that their spatial distribution is determined and they appeared "instantaneously", i.e. under the present spatial distribution of tracked satellites. This assumption is justified by the fact, that regions of greatest collision risk lies at altitudes, exceeding $800km$, where the influence of atmosphere on the objects more than $1cm$-sized, effects after tens and hundreds of years.

Real spatial and sizes distributions of untracked objects are not known well enough, and up to recent times, were practically absent. Thus, we shall make one more assumption, used in the environment model, developed in USA in 1989 (Ref.10). We shell suppose, that the spatial distribution of untracked breakup debris for arbitrary size coincides with the present distribution for tracked debris. We shall assume also, that spatial and sizes distribution of the future launched objects coincides with the present one for launch elements as well.

Appendix 4 presents annual collision probabilities for all considered objects, obtained under mentioned assumptions for different variants of non-tracked breakup debris, elements of future launches and breakups.These variants are as follows: 1-Russian catalog of tracked satellites (RCAT) 1992, 2-US catalog of tracked satellites (USCAT) 1992 (700 additional fragments with size $10cm$), 3-USCAT+3000fr(10) (fragments sizes up to $10cm$), 4-USCAT+3000fr(10)+5000fr(5), 5-USCAT+3000fr(10)+5000fr(5)+15000fr(3), 6-USCAT+3000fr(10)+5000fr(5)+15000fr(3)+40000fr(1), 7-Doubled amount of fragments with sizes more than $1cm$, a-current situation regarding launch elements, b-current situation+25% , c-current situation+50% , d-current situation+100% .

These data reveals, that annual probability of collision between objects with sizes more than $10cm$, is equal to 0.043, with sizes more than $1cm$-0.25. Doubling the amount of all types of objects, more than 1cm size, now resident in their orbits, the annual collision frequency will reach 1.

Figures 22-24 depicts the probability of collision between imaginary object and objects of environment, exceeding $1cm$ in size, in accordance with object size and altitude of circular orbit (inclinations regions $65° - 75°, 75° - 85°, 95° - 105°$). Technique, used to obtain the results,is the same as for figures 19-21. Method of non-tracked debris consideration is similar to the method, used to calculate the table for Appendix 4.
It is interesting to compare the data, presented in Fig.19-21 (no consideration of untracked objects) to Fig.22-24 (all the objects, with $d > 1cm$, including non-tracked, are taken into account). Here the increase of collision probability with increase of size of the launched object, is more noticeable. It is nearly quadratic. Collision probability for $10m$ sized object exceeds that for $1m$ sized by a factor of 50-80. Taking into account, that the sizes of majority of considered environment are much less than all reviewed sizes of launched object, we can explain the effect.

Consideration of untracked objects leads to increase of collision probability by a factor of 2.7 (for $d = 1m$) and 10 (for $d = 10m$). The greatest collision probability, as for previous cases, relates to the region $i = 75° - 85°, h850 - 950km$. For $1m$ size launched objects this probability, adjusted to annual, equals 0.68×10^{-4} . For $10m$ size the collision probability equals 0.45×10^{-2} .

5 Comparative analysis

This last section is devoted to comparison of space debris hazard averaged characteristics, obtained by direct method, and the method, developed by D.Kessler (Ref.2), based on employment of satellites spatial density. The basic relationships of this method are as follows.

Probability density function for a satellite in orbit, characterized by vector $E = (i, r_a, r_p)$, regarding spherical coordinates (r, φ, λ) is expressed by the formulas

$$f_0(r, \varphi, \lambda|E) = f_0(r, \varphi|E) = f_{01}(r|E) f_{02}(\varphi|E)$$

$$f_{01}(r|E) = (4\pi^4 r^{-2}(r_a + r_p)^2(r - r_p)(r_a - r))^{-0.5}$$
$$f_{02}(\varphi|E) = (0.25\pi^2 \cos^{-2}\varphi(\sin^2 i - \sin^2\varphi))^{-0.5} \quad (12)$$

where i - inclination, r_a, r_p - apogee and perigee distances respectively.

The function Eq.12 satisfies normalizing condition

$$\int_0^{2\pi} \int_{-i}^{i} \int_{r_p}^{r_a} f_0(r, \varphi, \lambda|E) dr d\varphi d\lambda = 1 \quad (13)$$

Probability density function $f(r, \varphi)$ for all n_t tracked objects is given by

$$f(r, \varphi) = \frac{1}{n_t} \sum_{i=1}^{n_t} f_0(r, \varphi|E_i) \quad (14)$$

Probability density Eq.14 also satisfies the normalizing condition, similar to Eq.13.

The spatial density of objects (per unit volume) thus is presented by

$$F(r, \varphi) = n_t \frac{f(r, \varphi)}{r^2 cos\varphi} \quad (15)$$

Considering the density F constant within a certain spatial region, probability of collision between imaginary object and all tracked satellites is determined by formula

$$P_c = FSv_{rel}\Delta t \qquad (16)$$

where S is collision cross-section, v_{rel} - average relative velocity, Δt - interval of object's residence in the region.

If a certain object within interval τ travels through the regions with variating according to r and φ spatial density, collision probability should be determined as follows

$$P_c(\tau) = \sum_{ij} p_{ij}$$

$$p_{ij} = F(r_i, \varphi_j) S_{ij} v_{rel}^{ij} \sum_{k=1}^{m_{ij}} \Delta t_{ijk} \qquad (17)$$

where Δt_{ijk} - intervals of residence in altitude-latitude region, characterized by r_i, φ_j; m_{ij} - number of passes through the region in the course of interval τ; S_{ij} and v_{rel}^{ij} - average collision cross-section and average relative velocity in the region, characterized by r_i, φ_j .

Eq.14,15 are used to calculate the spatial density of tracked objects. Probability of collision between an arbitrary object with chosen orbital parameters, and all the tracked satellites is calculated, according to Eq.17.

Figures 25 and 26 present the normalized altitude and latitude distributions of satellites, obtained by direct method and according to Eq.14, both applied to the same database. Calculations, based on Eq.14 were performed with the steps, equal to distribution steps for direct method.

The data presented demonstrate close coincidence of both methods. Higher maxima, and, respectively, lower minima of latitude distribution, produced by technique of D.Kessler, are caused by existence of singularities in Eq.14 at $\varphi = i$, which cannot be adequately represented by the data, obtained by direct method.

Figures 27-32 demonstrate annual probability of collision between a satellite of size d, launched to circular orbit of inclination i and altitude h, and all tracked satellites. It was calculated according to three different techniques:
- direct method (see also Figs.19,20,21);
- formula Eq.17, taking $S_{ij} = 0.25\pi d^2, v_{rel}^{ij} = 10km/s$;
- formula Eq.17, taking $S_{ij} = 0.25\pi(d + d(r_i, \varphi j))^2$, $v_{rel}^{ij} = v_{rel}(r_i, \varphi_j)$

where $d(r_i, \varphi j)$ and $v_{rel}(r_i, \varphi_j)$ are the averaged sizes and relative velocities in the vicinity of r_i, φ_j , obtained by direct method. Data are presented in dependence of altitude, for inclinations $74.0, 81.2, 95.1$ and sizes $2m, 7m$.

As evident from figures 27-32, the employment of analytical technique of D.Kessler, using constant value $10km/s$ for relative velocity and without consideration of sizes of tracked objects, results in underestimation of collision probability up to a factor of three.

But taking into account real spatial distributions of sizes and relative velocities leads to satisfactory agreement with direct method. Discrepancies, as a rule, do not exceed 20%. Still, for certain points of the plots, they are greater,that can be the result of either a different distribution step for the data, obtained by direct method, or incompleteness in consideration details of real satellites distribution in sizes,present in D.Kessler's technique. The first reason corresponds to the region of $i = 95.1°, h = 1000km$, and the second - to the region $i = 81.2°, h = 900km$, where we can see a jam of large satellites.

Thus, provided the tuning of D.Kessler's technique with the help of data, obtained in executing the direct method, we can see, that two conceptually different approaches - direct and based on the concept of spatial density,being exercised on the same database, produce close results, regarding collision probability for hypothetical object.

6 Acknowledgements

Vasily Smelov and Oleg Nazin developed the computer code, realizing direct method; Georgy Mahonin was the key figure in "rapid" prediction procedures; Alexander Feoktistov and Igor Kostin made valuable contributions to computer realization and tuning of the spatial density based techniques; Alexey Kourenshikov carefully performed the plots, presented in the paper; Olga Vorotniuk and Natalia Turina assisted with computer runs.

7 References

1.Johnson N.L., McKnight D.S.,*Artificial Space Debris*,Orbit Book Company, Malabar, Fl,1991.

2.Kessler D.J., "Derivation of the Collision Probability between Orbiting Objects: The Lifetime of Jupiter's Outer Moons", *ICARUS*,Vol.48,1981,pp.39-48.

3.Eichler,P.and D.Rex,"Debris Chain Reactions",Paper AIAA-90-1365,presented at AIAA/NASA/DOD *Orbital Debris Conference* and Future Directions, April 16-19,1990.

4.Vedder J.D. and J.L.Tabor, "New Method for Estimating Low - Earth - Orbit Collision Probabilities", *Journal of Spacecraft and Rockets*, Vol.28, N 2, 1991, pp 210-215.

5.В.Ф.Бойков,и др., "Быстродействующие алгоритмы прогнозирования
движения для оперативного уточнения параметров и времени существования космических об'ектов",*Наблюдения искусственных небесных тел*, N 84, часть 1, Москва 1988, стр.81-89.

6.В.Ф.Бойков,и др., "Повышение точности быстродействующего алгоритма прогнозирования движения ИСЗ", *Наблюдения искусственных небесных тел*, N 86,часть 1, Москва 1990, стр.64-73.

7.З.Н.Хуторовский, "Ведение каталога космических об'ектов, технология и результаты исследований", *Космические исследования*,- in press.

8.Г.Н.Дубошин, Небесная механика. Основные задачи и методы, Наука, 1968.

9.Dicky V.I.,et al., "Russian Space Surveillance System and Some Estimations of Safe Activity in Space on the Base of its Information", presented at *World Space Congress*, Washington, DC, September, 1992.

10.Kessler D.J.,et al.,*Orbital Debris Environment for Spacecraft Designed to Operate in Low Earth Orbit*, NASA TM 100-471, April,1989.

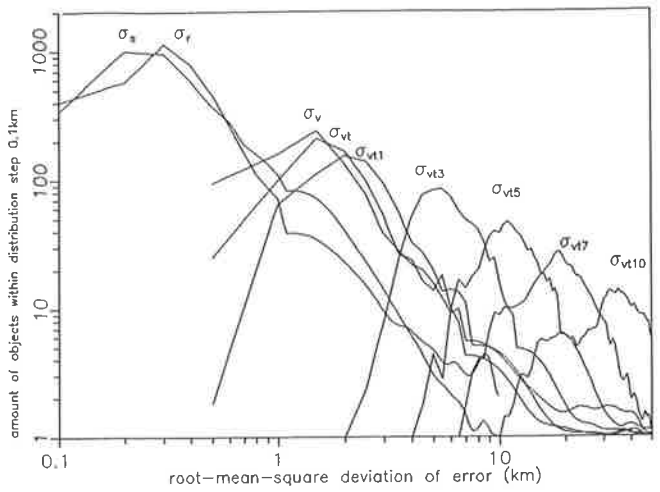

Fig.1 Distribution of satellites according to root-mean-square deviation of errors (orbital coordinate system considered): along the position vector(σ_r); in lateral direction(σ_s); in transversal direction: σ_v-for the moment of the last refinement, σ_{vt}-regarding prediction to the current moment t, σ_{vti}-to the moment t+i (i=1,2,3,5,7,10).

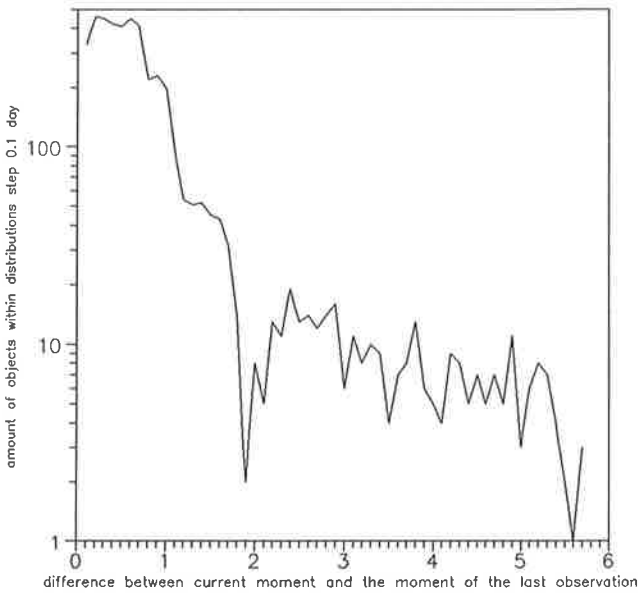

Fig.2 Distributions of satellites according to the value of the difference between current moment and time reference of the element set, concident with the moment of the last observation

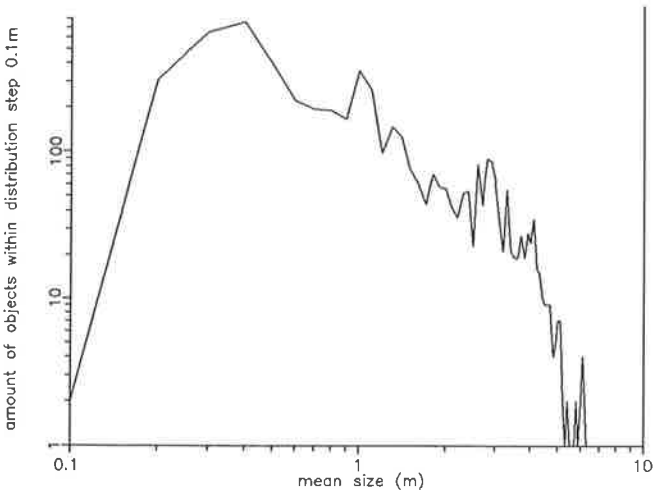

Fig.3 Distribution of satellites in obtained from radar cross-section mean size (70 cm wavelength signal)

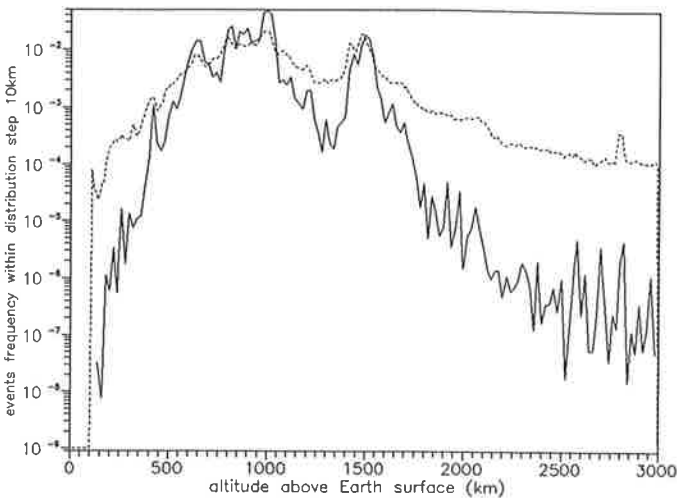

Fig.4 Normalized altitude distribution of satellites (short-dashes line) and collision probabilities (solid line)

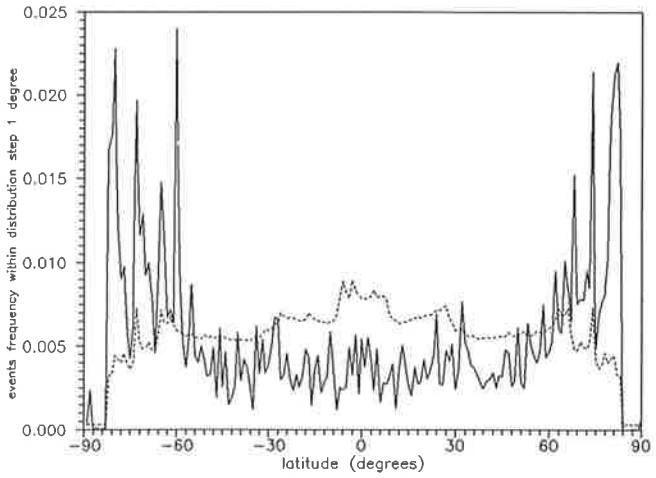

Fig.5 Normalized latitude distribution of satellites (short-dashes line) and collision probabilities (solid line)

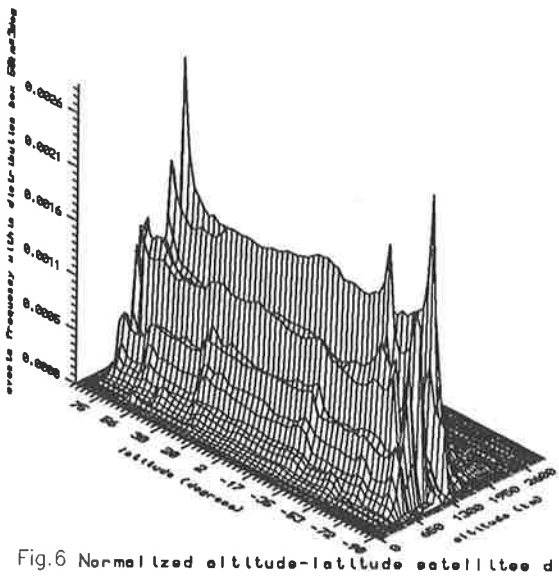

Fig.6 Normalized altitude-latitude satellites distribution

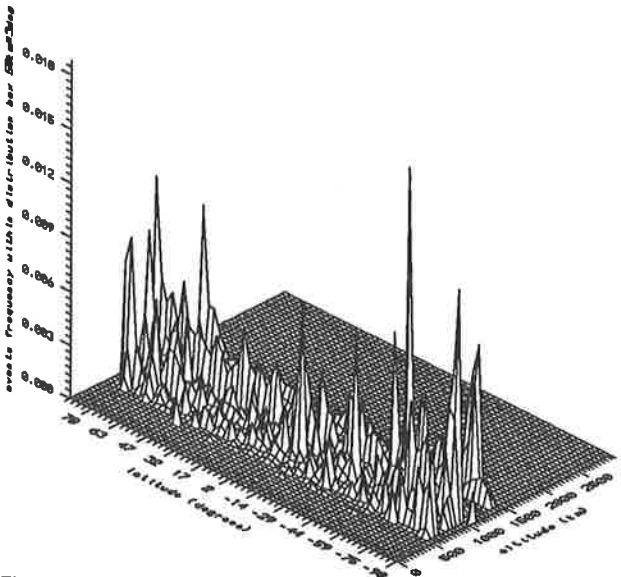

Fig.7 Normalized altitude-latitude collision probability distribution

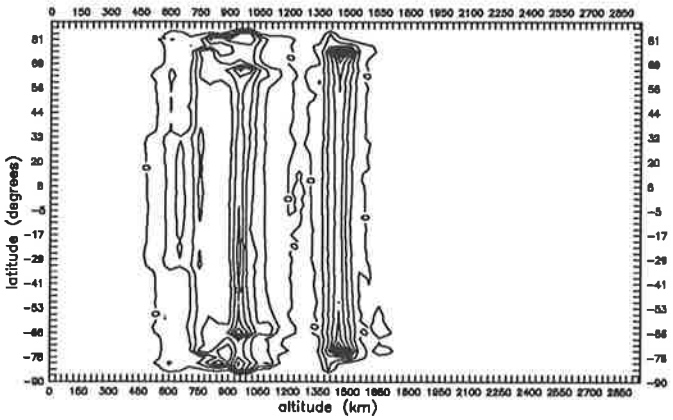

Fig.8 Topographic projection of satellites altitude-latitude distribution (level curves step 0.0003)

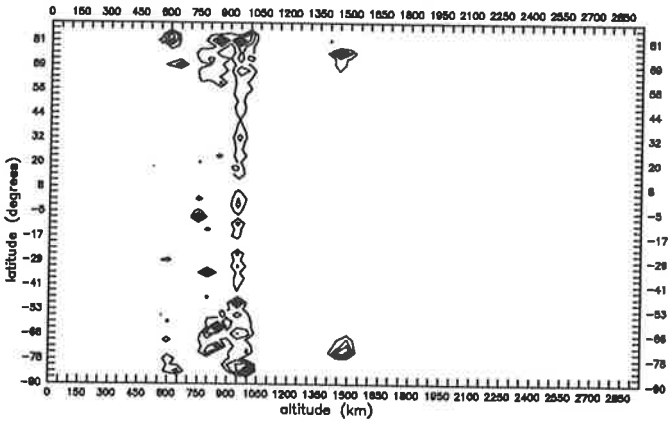

Fig.9 Topographic projection of collision probability altitude-latitude distribution (level curves step 0.002)

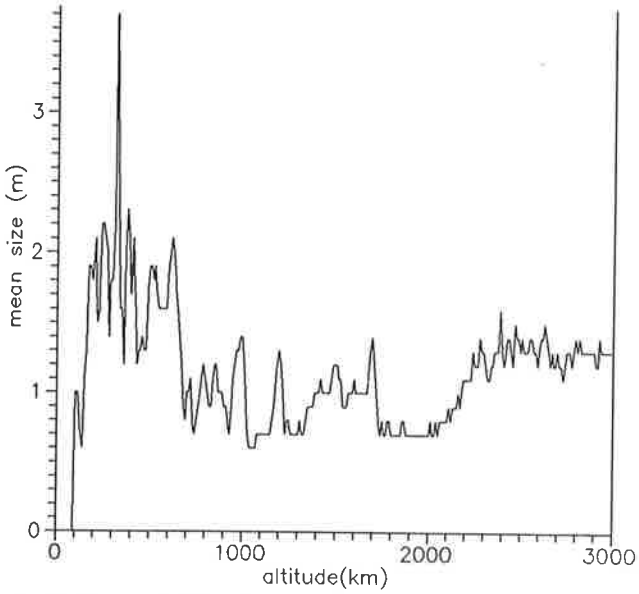

Fig.10 Mean satellite size as a function of altitude (10km – wide averaging intervals)

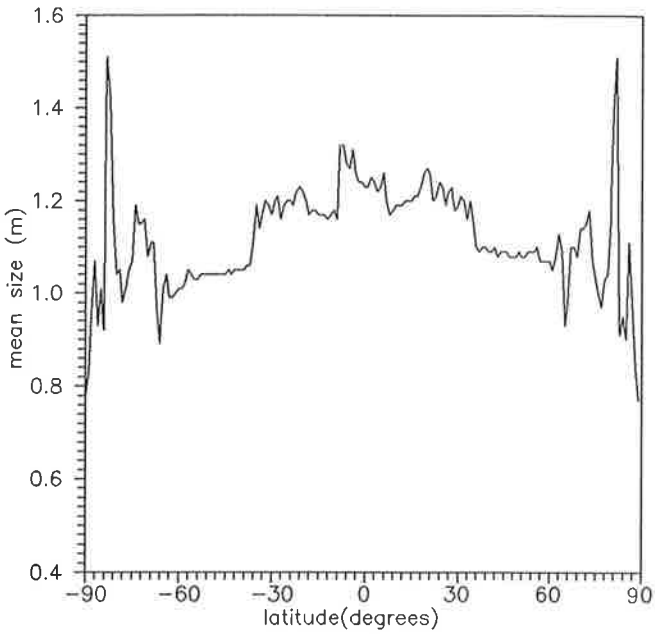

Fig.11 Mean satellite size as a function of latitude (1 degree – wide averaging intervals)

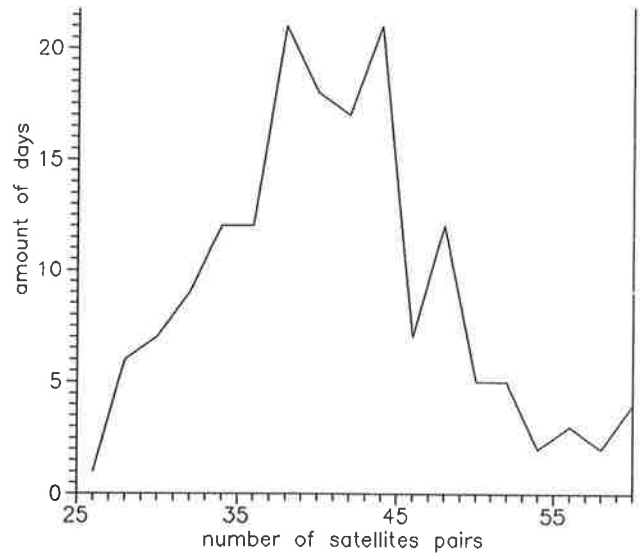

Fig.12 Distribution of amount of days (a year) in accordance with the number of satellite's pairs having approach distance less than 1km(for a day)

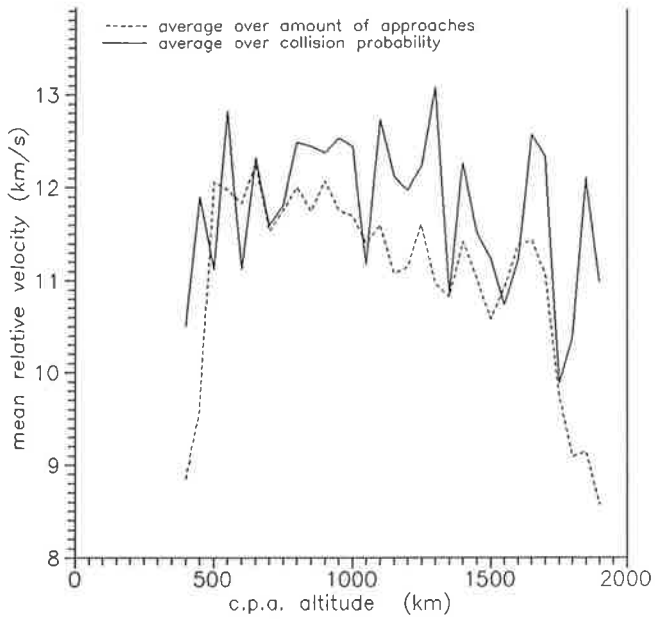

Fig.13 Mean relative velocity for two approaching satellites as a function of c.p.a. altitude (50km – wide averaging intervals)

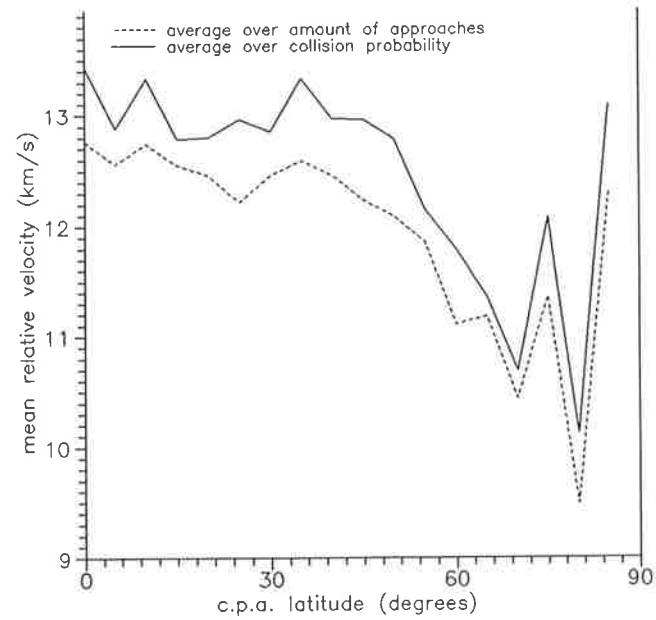

Fig.14 Mean relative velocity for two approaching satellites as a function of c.p.a. latitude (5 degrees – wide averaging intervals)

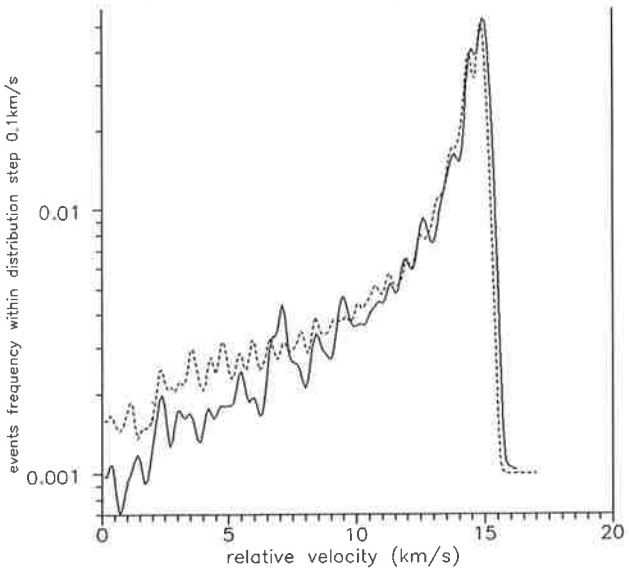

Fig.15 Normalized distributions of the number of satellite's approaches (short–dashes line) and collision probability (solid line) according to relative velocity

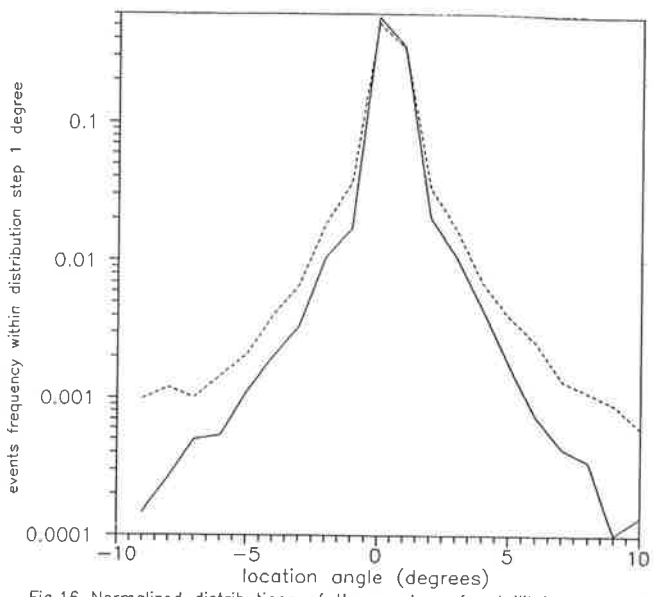

Fig.16 Normalized distributions of the number of satellite's approaches (short–dashes line) and collision probability (solid line) according to location angle in orbital biconical coordinate system

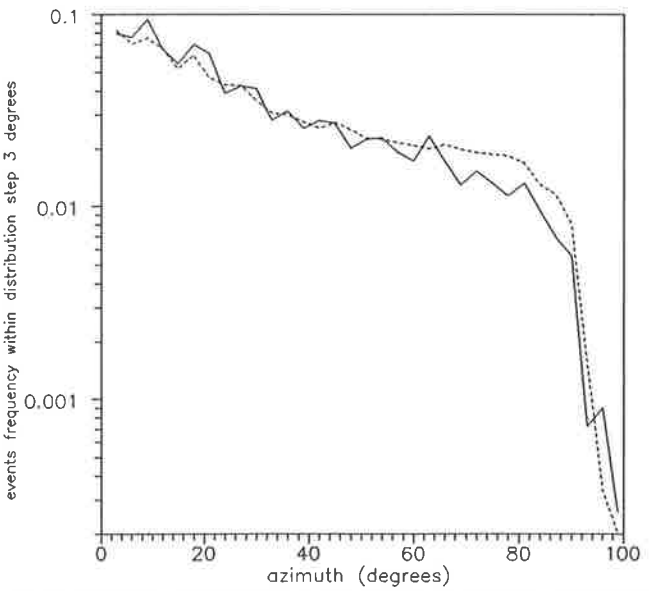

Fig.17 Normalized distributions of the number of satellite's approaches (short–dashes line) and collision probability (solid line) according to azimuth in orbital biconical coordinate system

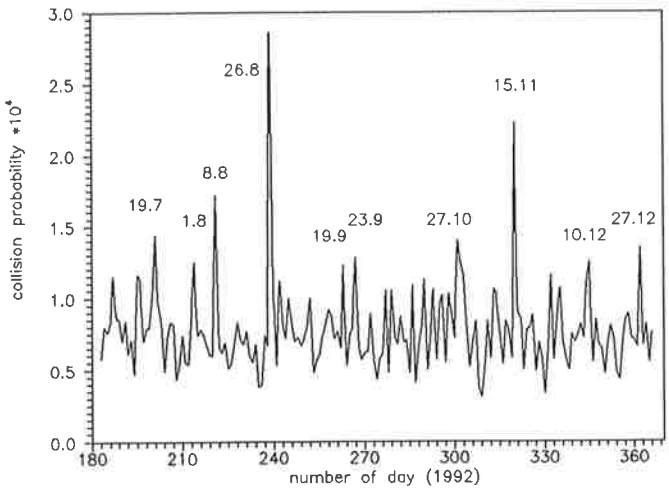

Fig.18 Daily collision probability variations during second half of 1992 (all tracked satellites considered).Major maximums correspond to the days, when the most dangerous approaches occurred

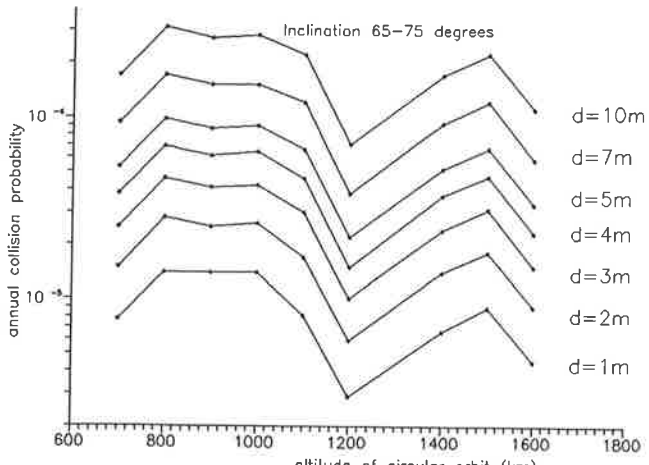

Fig.19 Altitude and size dependence of collision probability for a satellite in a circular orbit with inclination inside 65–75 interval (all tracked satellites considered)

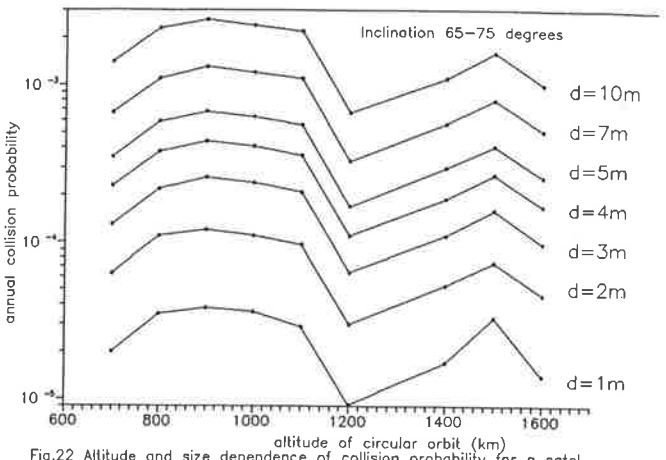

Fig.22 Altitude and size dependence of collision probability for a satellite in a circular orbit with inclination inside 65–75 interval (considering all satellites, sized more than 1 cm)

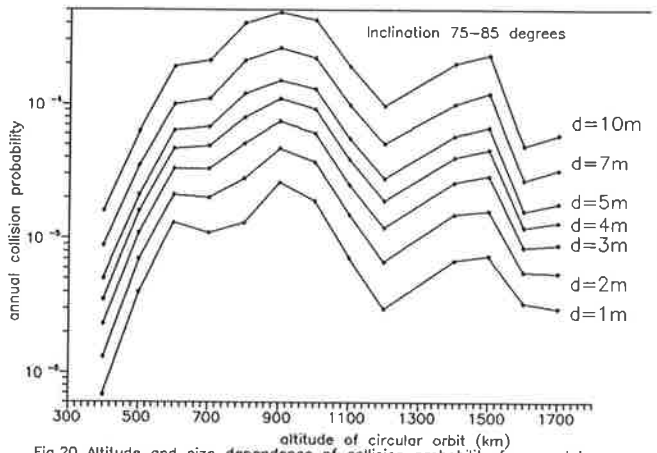

Fig.20 Altitude and size dependence of collision probability for a satellite in a circular orbit with inclination inside 75–85 interval (all tracked satellites considered)

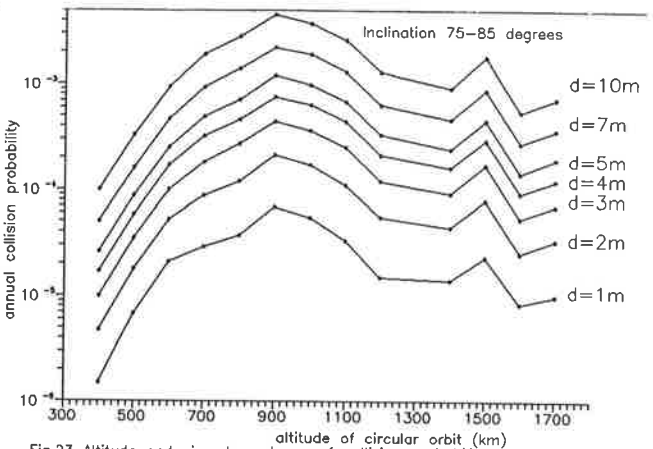

Fig.23 Altitude and size dependence of collision probability for a satellite in a circular orbit with inclination inside 75–85 interval (considering all satellites, sized more than 1 cm)

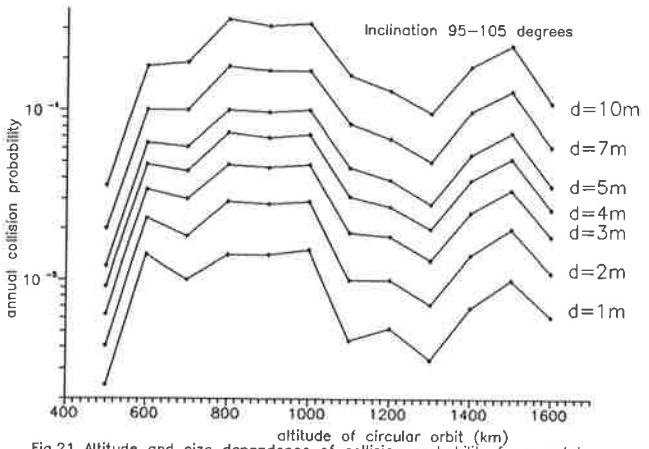

Fig.21 Altitude and size dependence of collision probability for a satellite in a circular orbit with inclination inside 95–105 interval (all tracked satellites considered)

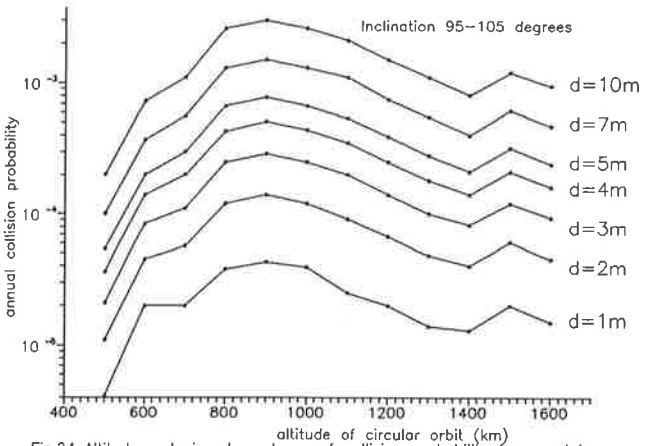

Fig.24 Altitude and size dependence of collision probability for a satellite in a circular orbit with inclination inside 95–105 interval (considering all satellites, sized more than 1 cm)

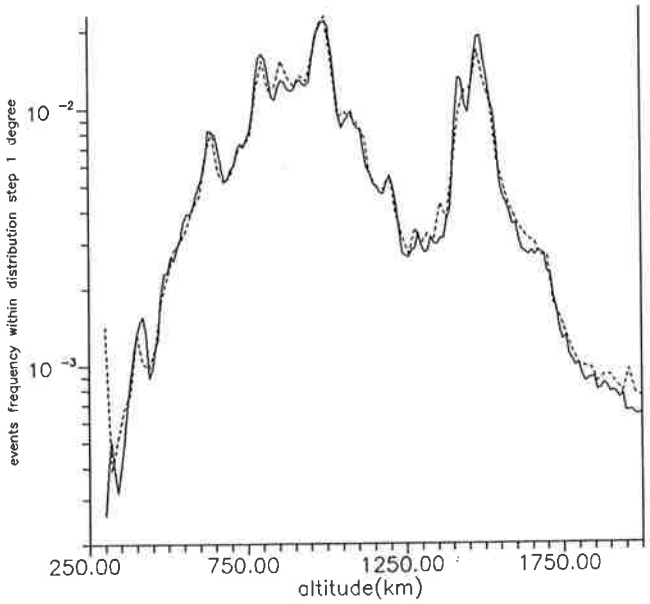

Fig.25 Normalized altitude distribution of satellites, obtained by direct method (solid line) and D.Kessler's method (short-dashes line)

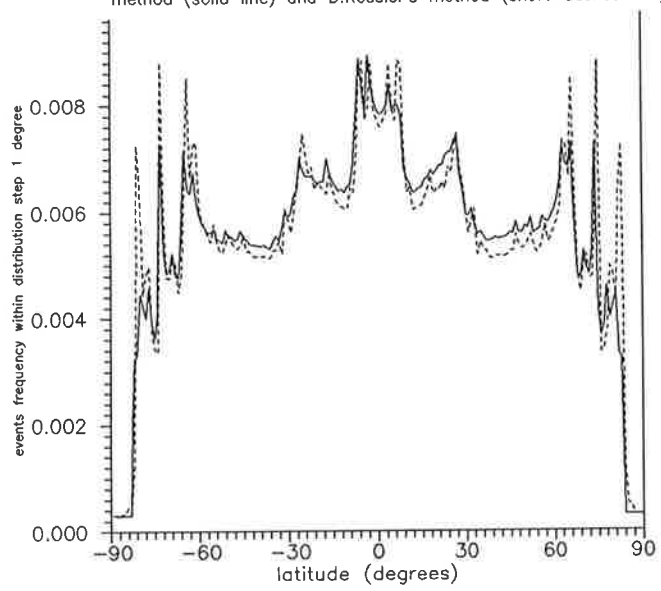

Fig.26 Normalized latitude distribution of satellites, obtained by direct method (solid line) and D.Kessler's method (short-dashes line)

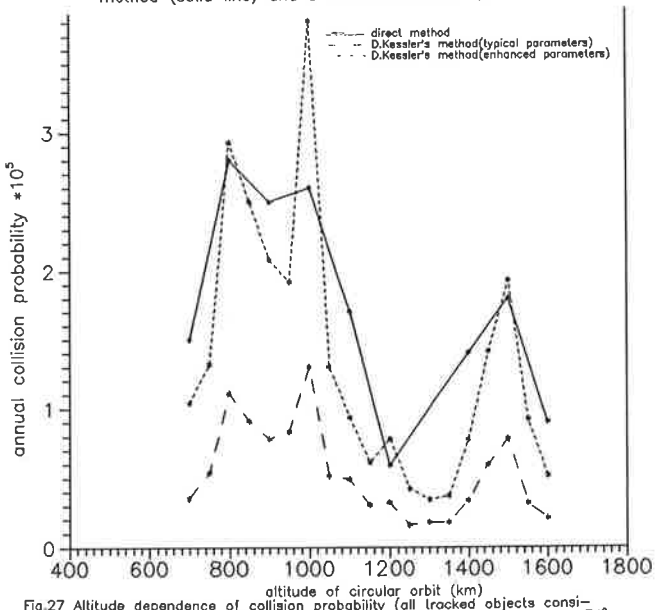

Fig.27 Altitude dependence of collision probability (all tracked objects considered) for a 2-m sized satellite in a circular orbit with inclination 74°

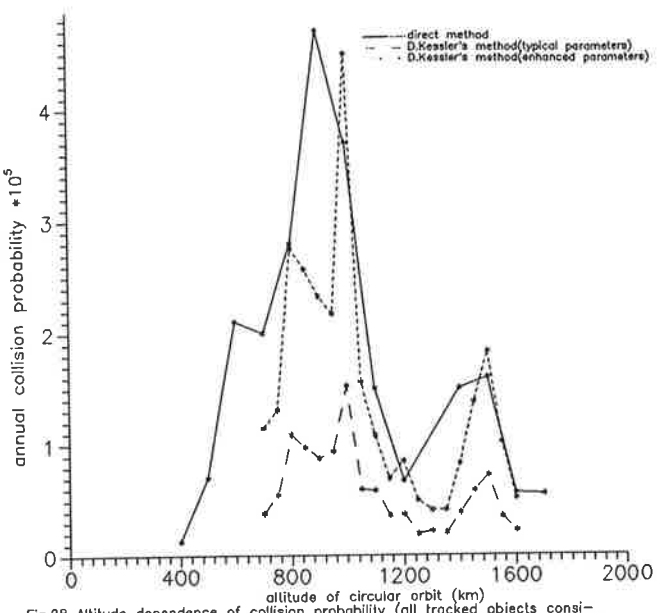

Fig.28 Altitude dependence of collision probability (all tracked objects considered) for a 2-m sized satellite in a circular orbit with inclination 81°

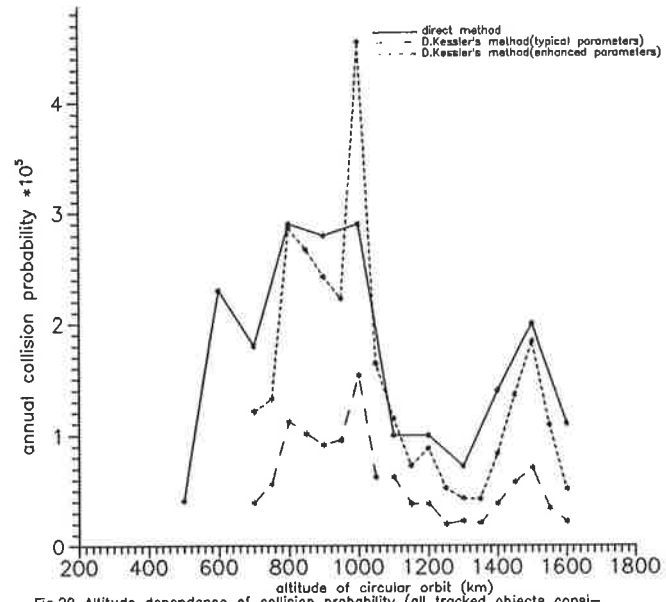

Fig.29 Altitude dependence of collision probability (all tracked objects considered) for a 2-m sized satellite in a circular orbit with inclination 95°

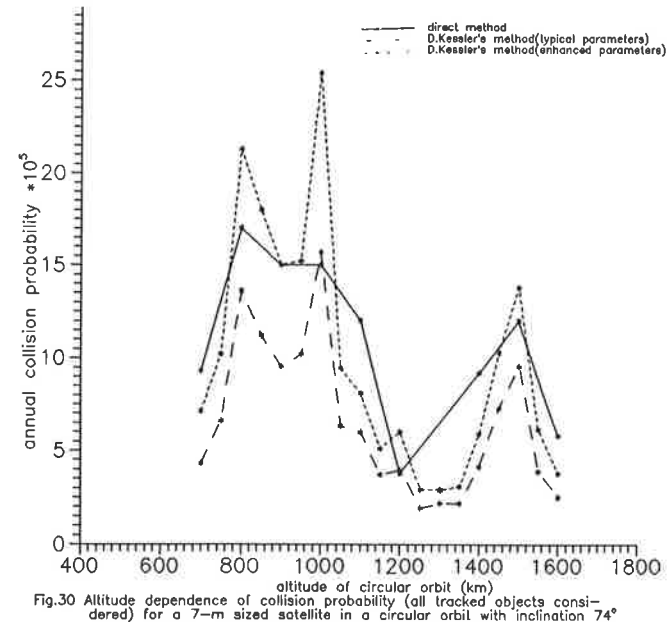

Fig.30 Altitude dependence of collision probability (all tracked objects considered) for a 7-m sized satellite in a circular orbit with inclination 74°

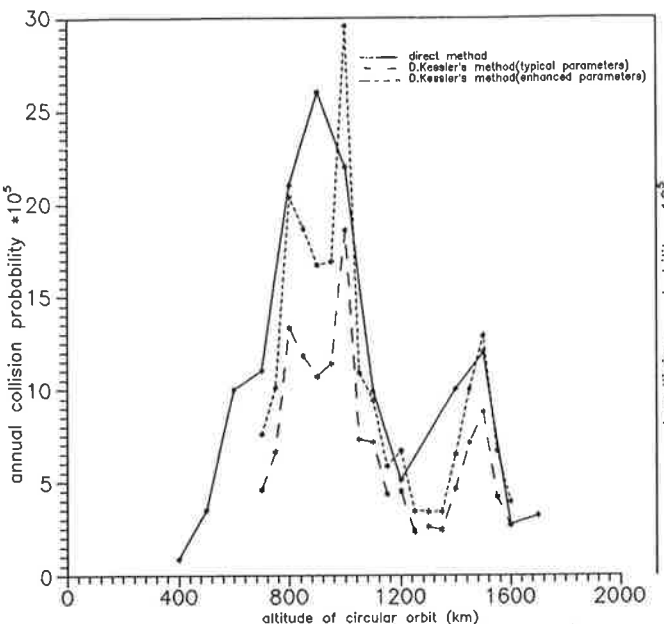

Fig.31 Altitude dependence of collision probability (all tracked objects considered) for a 7–m sized satellite in a circular orbit with inclination 81°

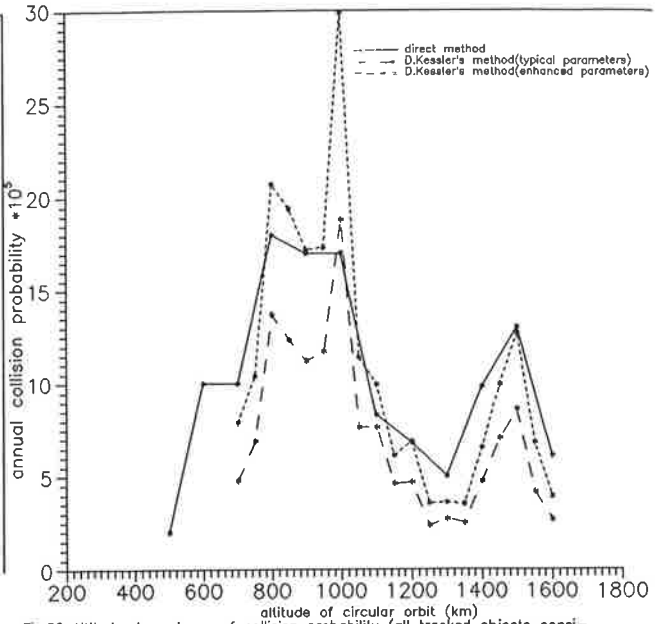

Fig.32 Altitude dependence of collision probability (all tracked objects considered) for a 7–m sized satellite in a circular orbit with inclination 95°

$\Delta\rho$	0.1km	0.2km	0.3km	0.5km	1km	2km	3km
n_p	0.65	2.7	4.1	10.7	41.6	166	375

Table 1. Daily averaged number of satellite pairs.

h_{km}	350 ÷	450 ÷	550 ÷	650 ÷	750 ÷	850 ÷	950 ÷	1050 ÷	1150 ÷	1250 ÷	1350 ÷	1450 ÷	1550 ÷	1650 ÷
i°	450	550	650	750	850	950	1050	1150	1250	1350	1450	1550	1650	1750
65÷75	2	4	2	19	119	63	57	4	12	0	86	294	74	1
75÷85	5	28	112	19	6	62	276	2	21	0	83	16	3	9
95÷105	1	8	19	23	86	55	13	18	9	3	27	69	28	28

Table 2. Amounts of objects in (i, h)-regions.

p_1, p_2	$1,10^{-5}$	$10^{-5}, 10^{-6}$	$10^{-6}, 10^{-7}$	$10^{-7}, 10^{-8}$	$10^{-8}, 10^{-9}$	$10^{-9}, 10^{-10}$	$10^{-10}, 10^{-11}$
$\overline{n}_c$	0.78	13	71	204	424	540	473

Table 3. Daily number of approaches distribution.

NN	Intern. designa-tors	Types	Coun try	Si-zes	Root-mean square errors	Incl.	Altitudes	Moment of approach	Dis-tance	Rel. velo city	Alt	Lat	Colli-sion prob.
1	2	3	4	5	6	7	8	9	10	11	12	13	14
1	74-25-1	Meteor-1	CIS	2,8	0,2 0,1 0,1	81,2	897/857	26.08.92	0,1	14,1	883	-61	$0,24*10^{-3}$
	75-124-1	Meteor-1	CIS	2,7	0,5 0,1 0,1	81,2	897/848	01.59.31,55	(0,0)				
2	88-102-2	Cosmos-1980 R/B	CIS	4,6	0,6 0,1 0,1	71,0	873/833	15.11.92	0,1	14,2	849	-36	$0,11*10^{-3}$
	72-22-2	Meteor-1 R/B	CIS	3,4	0,2 0,1 0,1	81,2	924/840	03.41.38,04	(0,1)				
3	79-57-1	NOAA-2	USA	2,4	0,3 0,1 0,1	98,6	824/791	08.08.92	0,0	14,9	793	-8	$0,11*10^{-3}$
	72-43-1	Cosmos-494	CIS	1,3	0,6 0,1 0,1	74,1	809/776	19.31.46,95	(0,0)				
4	90-86-1	Meteor-2	CIS	2,8	0,6 0,1 0,1	82,5	989/947	27.12.92	0,1	14,4	973	-51	$0,11*10^{-3}$
	72-62-2	Cosmos-514 R/B	CIS	2,3	0,6 0,1 0,1	83,0	989/952	07.43.30,54	(0,1)				
5	91-17-1	Lacross-2	USA	8,4	0,8 0,1 0,1	68,0	693/668	27.10.92	0,6	11,6	682	68	$0,77*10^{-4}$
	90-43-7	Maksat DEB	USA	0,2	0,7 0,1 0,1	89,9	696/574	19.02.45,81	(0,0)				
6	83-4-1	IRAS	Neth	3,1	1,5 0,1 0,2	99,0	932/892	10.12.92	0,3	14,7	931	-81	$0,64*10^{-4}$
	76-43-2	Meteor-2 R/B	CIS	2,9	1,0 0,1 0,1	81,2	932/841	06.28.22,00	(0,0)				
7	88-78-1	Ferret	USA	4,1	0,3 0,1 0,1	85,0	817/789	23.09.92	0,1	13,2	814	-66	$0,54*10^{-4}$
	76-69-1	Cosmos-841	CIS	1,3	0,3 0,1 0,1	74,0	816/776	14.51.25,51	(0,1)				
8	79-95-1	Meteor-2	CIS	3,8	0,4 0,1 0,1	81,2	909/870	01.08.92	0,1	12,4	874	58	$0,51*10^{-4}$
	75-25-1	Cosmos-724	CIS	1,7	0,8 0,1 0,1	65,6	956/873	17.13.05,96	(0,0)				
9	83-4-2	PIKS-2	USA	3,9	2,1 0,3 0,2	100,0	898/856	01.09.92	0,2	14,8	884	80	$0,39*10^{-4}$
	64-51-2	Explorer-20 R/B	USA	1,4	1,0 0,1 0,1	79,9	999/850	02.03.47,72	(0,1)				
10	79-32-2	Cosmos-1093 R/B	CIS	4,2	1,9 0,2 0,1	81,2	612/526	16.10.92	0,3	15,1	609	-78	$0,87*10^{-4}$
	77-57-2	Meteor-2 R/B	CIS	2,1	2,2 0,1 0,1	97,9	607/579	03.55.19,79	(0,1)				
11	74-25-2	Meteor-1 R/B	CIS	2,9	1,1 0,1 0,1	81,2	944/845	19.09.92	0,2	12,4	935	-56	$0,32*10^{-4}$
	82-43-1	Cosmos-1365	CIS	2,1	0,7 0,1 0,1	65,1	975/893	13.35.24,07	(0,1)				
12	88-46-1	Cosmos-1950	CIS	4,7	0,9 0,1 0,1	73,6	1534/1503	19.07.92	0,4	7,0	1510	-71	$0,32*10^{-4}$
	92-30-7	Cosmos-2193	CIS	1,0	0,5 0,1 0,1	74,0	1512/1476	01.24.44,99	(0,0)				
13	83-10-2	Cosmos 1441 R/B	CIS	2,1	1,7 0,1 0,1	81,1	653/567	15.08.92	0,1	13,1	599	80	$0,31*10^{-4}$
	79-5-1	Meteor-2	CIS	3,1	1,4 0,1 0,1	97,7	609/556	06.02.50,15	(0,0)				
14	82-59-1	Cosmos-1378 R/B	CIS	5,0	1,7 0.2 0,1	82,5	650/601	01.11.92	0,2	14,5	649	-59	$0,31*10^{-4}$
	86-18-2	Cosmos-1733 R/B	CIS	2,6	1,3 0,1 0,1	82,5	661/624	21.06.13,18	(0,2)				
15	79-90-2	Cosmos-1141 R/B	CIS	3,0	0,6 0,1 0,1	82,9	999/957	15.11.92	0,3	13,9	963	-33	$0,30*10^{-4}$
	84-112-1	Cosmos-1607	CIS	1,8	0,6 0,1 0,1	65,0	995/935	18.29.52,39	(0,1)				
16	81-91-2	Cosmos-1308 R/B	CIS	3,4	1,6 0,1 0,1	82,9	1017/963	19.10.92	0,1	14,4	10^{3}	-11	$0,30*10^{-4}$
	71-111-1	Cosmos-465	CIS	2,9	1,4 0,1 0,1	74,0	1010/963	16.05.14,79	(0,1)				
17	81-117-1	Cosmos-1328	CIS	3,1	0,3 0,1 0,1	82,5	655/609	29.08.92	0,1	9,2	614	80	$0,29*10^{-4}$
	80-8-2	Cosmos-1154 R/B	CIS	4,6	0,7 0,1 0,1	81,2	615/553	16.07.44,83	(0,1)				
18	81-43-1	Meteor-2	CIS	3,4	0,4 0,1 0,1	81,3	924/836	28.10.92	0,2	14,8	910	81	$0,29*10^{-4}$
	90-81-12	Fengyun-2 DEB	PRC	0,8	1,2 0,4 0,3	98,9	910/885	13.10.24,11	(0,1)				
19	84-56-2	Cosmos-1570 R/B	CIS	2,6	1,9 0,1 0,1	74,1	808/778	16.10.92	0,3	14,9	779	-4	$0,27*10^{-4}$
	71-87-1	DMS	USA	1,0	2,6 0,1 0,1	99,2	856/779	05.25.04,14	(0,1)				
20	78-31-2	Cosmos-996 R/B	CIS	3,5	0,7 0,1 0,1	82,9	1027/958	12.11.92	1,1	8,1	959	81	$0,27*10^{-4}$
	82-25-2	Meteor-2 R/B	CIS	3,0	0,9 0,1 0,1	82,5	979/940	02.30.22,19	(0,0)				

APPENDIX 2.

NN	Intern. designi-tor	Type	Si-ze (m)	Incl	Alti-tudes	Moment of approach	Dis-tance	Relat. velo-city	C.p.a. alti-tude	C.p.a. lati-tude	Ang-le A	Ang-le B	Collision probabi-lity
1	2	3	4	5	6	7	8	9	10	11	12	13	14
1	66-70-4	OV-3-3 DEB	0,3	81,5	3549 417	20.07.92 01.15.38,4	22,3 4,6	14,0	410	32,5	30,1	-0,2	$0,13*10^{-8}$
2	91-5-1	Cosmos-2122	3,7	65,0	429 411	23.07.92 19.28.48,0	10,6 0,1	12,9	412	-10,4	32,3	0,0	$0,27*10^{-6}$
3	91-5-1	Cosmos-2122	3,7	65,0	429 411	23.07.92 21.01.31,6	8,5 0,0	12,9	412	-10,6	32,3	0,0	$0,13*10^{-5}$
4	–	–	4,4	34,5	15716 184	28.08.92 14.02.11,1	29,1 5,2	10,4	413	-23,1	60,7	8,0	$0,57*10^{-7}$
5	–	–	1,0	7,4	29163 318	29.08.92 06.08.27,9	17,1 17,0	8,7	406	7,4	74,0	7,4	$0,28*10^{-8}$
6	84-68-1	Cosmos-1578	1,8	50,6	538 247	10.09.92 02.53.53,8	10,1 4,1	11,9	407	2,7	38,8	0,8	$0,14*10^{-6}$
7	87-30-1	Kvant-1	1,1	51,6	416 395	11.09.92 23.13.57,0	9,9 5,6	4,2	404	49,7	74,1	- 0,2	$0,39*10^{-10}$
8	91-5-1	Cosmos-2122	3,7	65,0	428 412	12.09.92 10.47.13,2	3,6 0,8	8,9	421	-48,2	54,1	0,0	$0,17*10^{-5}$
9	–	–	1,1	52,0	18713 407	17.10.92 19.04.33,8	5,3 5,1	13,6	403	5,7	43,5	0,6	$0,20*10^{-8}$
10	–	–	1,1	65,0	433 409	27.10.92 11.46.07,0	8,9 8,6	2,6	405	38,2	80,0	0,1	$0,35*10^{-8}$
11	–	–	2,0	7,4	30699 300	02.11.92 22.09.55,7	13,3 13,3	8,6	402	5,4	75,3	7,1	$0,12*10^{-8}$
12	83-111-1	Cosmos-1508	2,5	82,9	1806 399	08.11.92 10.18.01,2	0,3 0,3	12,7	403	45,2	36,9	0,2	$0,21*10^{-4}$
13	–	–	0,6	26,8	11707 352	09.11.92 09.16.19,7	4,4 4,3	8,9	399	22,3	67,1	3,9	$0,73*10^{-8}$
14	–	–	0,4	26,7	2014 248	10.11.92 06.47.55,6	14,9 14,8	9,5	399	12,3	54,4	-3,4	$0,47*10^{-8}$
15	–	–	1,3	6,2	7321 134	11.11.92 18.09.32,3	20,3 10,7	10,7	401	-5,5	74,0	-10,7	$0,81*10^{-8}$
16	72-23-6	Cosmos-482 DEB	1,0	52,1	6342 220	15.11.92 11.19.05,6	13,1 6,1	7,8	409	-45,6	68,9	-7,4	$0,29*10^{-8}$
17	87-12-7	Astro-3 DEB	0,5	30,8	413 369	17.11.92 16.37.34,8	2,2 1,8	7,7	399	27,3	59,8	0,2	$0,40*10^{-8}$
18	–	–	0,2	65,7	627 434	18.11.92 11.49.54,7	22,8 15,4	11,6	412	-37,3	41,3	0,2	$0,15*10^{-8}$
19	–	–	1,1	65,0	431 410	19.11.92 01.23.28,9	8,6 8,2	2,8	413	-40,7	79,3	0,0	$0,14*10^{-8}$
20	–	–	6,1	32,2	426 408	22.11.92 14.34.46,5	28,3 8,1	9,2	413	-20,4	53,0	0,1	$0,58*10^{-10}$
21	–	–	3,0	41,2	5911 305	01.12.92 10.46.23,3	3,7 2,0	9,4	406	-31,9	59,7	-4,4	$0,63*10^{-7}$
22	–	–	0,4	26,7	2014 248	01.12.92 13.44.03,0	13,8 3,4	9,6	400	-11,1	54,1	-3,2	$0,12*10^{-7}$
23	–	–	2,8	37,4	5867 164	03.12.92 13.38.33,5	26,5 10,4	7,6	409	-34,9	69,1	8,2	$0,15*10^{-9}$
24	–	–	1,0	17,4	25203 415	11.12.92 21.00.05,9	28,4 22,6	5,6	398	5,1	93,9	1,4	$0,90*10^{-9}$
25	73-78-3	Explorer-50 DEB	2,2	28,8	862 322	26.12.92 12.58.40,0	14,4 3,5	9,9	392	-6,8	50,7	1,3	$0,70*10^{-8}$

APPENDIX 4.

	1	2	3	4	5	6	7
a	0.030	0.032	0.043	0.060	0.112	0.247	0.48
b	0.043	0.046	0.060	0.081	0.145	0.313	0.58
c	0.059	0.062	0.079	0.104	0.181	0.382	0.70
d	0.097	0.102	0.123	0.158	0.260	0.526	0.97

APPENDIX 3.

N	designa-tor	Type	Size	Incl.	Altitudes	Amount	collision probabil.
1	2	3	4	5	6	7	8
1	75-124-1	Meteor-1	3.1	81.2	890/849	207	$0.26*10^{-3}$
2	74-25-1	Meteor-1	2.6	81.2	901/856	150	$0.26*10^{-3}$
3	88-102-2	Cosmos-1980 R/B	4.8	71.0	878/838	179	$0.17*10^{-3}$
4	72-22-2	Meteor-1 R/B	3.1	81.2	923/838	161	$0.15*10^{-3}$
5	79-57-1	NOAA-2-1	2.6	98.6	817/798	182	$0.14*10^{-3}$
6	72-62-2	Cosmos-514 R/B	2.6	83.0	986/952	231	$0.13*10^{-3}$
7	90-86-1	Meteor-2	4.3	82.5	990/949	152	$0.12*10^{-3}$
8	72-43-1	Cosmos-494	1.3	74.1	814/776	200	$0.11*10^{-3}$
9	88-46-1	Cosmos-1950	4.8	73.6	1540/1486	130	$0.92*10^{-4}$
10	91-17-1	Lacrosse-2	7.8	68.0	691/668	66	$0.88*10^{-4}$
11	79-95-1	Meteor-2	4.2	81.2	907/868	178	$0.87*10^{-4}$
12	90-57-1	Meteor-2	2.1	82.6	977/940	156	$0.85*10^{-4}$
13	90-43-7	Maksat DEB	0.2	89.9	719/580	81	$0.82*10^{-4}$
14	85-13-2	Meteor-2 R/B	2.6	82.5	987/942	158	$0.80*10^{-4}$
15	76-43-2	Meteor-2 R/B	2.6	81.2	920/834	171	$0.79*10^{-4}$
16	83-4-1	IRAS	2.4	99.0	922/892	164	$0.79*10^{-4}$
17	74-25-2	Meteor-1 R/B	2.7	81.2	939/838	187	$0.78*10^{-4}$
18	92-30-7	Cosmos-2193	1.0	74.0	1501/1475	119	$0.75*10^{-4}$
19	75-25-1	Cosmos-724	1.4	65.6	944/859	134	$0.73*10^{-4}$
20	82-25-2	Meteor-2 R/B	2.5	82.6	982/940	171	$0.72*10^{-4}$
21	88-78-1	Ferret	4.2	85.0	816/789	165	$0.71*10^{-4}$
22	82-59-1	Cosmos-1378	5.2	82.5	637/611	106	$0.70*10^{-4}$
23	83-4-2	PIKS-2	3.6	100.0	893/857	170	$0.67*10^{-4}$
24	76-69-1	Cosmos-841	1.3	74.0	807/774	166	$0.66*10^{-4}$
25	88-62-2	Cosmos-1959 R/B	3.5	82.9	1019/957	226	$0.65*10^{-4}$
26	80-99-2	Cosmos-1226 R/B	2.8	82.9	1010/966	197	$0.65*10^{-4}$
27	78-31-2	Cosmos-996 R/B	3.1	82.9	1011/963	240	$0.63*10^{-4}$
28	75-103-2	Cosmos-778 R/B	2.4	83.0	1014/963	209	$0.62*10^{-4}$
29	87-41-2	Cosmos-1844 R/B	3.7	71.0	861/831	157	$0.61*10^{-4}$
30	70-113-1	Cosmos-389	3.1	81.2	601/552	95	$0.59*10^{-4}$
31	77-122-2	Cosmos-971 R/B	3.0	82.9	1026/976	174	$0.58*10^{-4}$
32	79-90-2	Cosmos-1141 R/B	2.8	82.9	1019/959	180	$0.58*10^{-4}$
33	84-27-1	Cosmos-1544	4.8	82.6	635/601	97	$0.57*10^{-4}$
34	75-28-2	Cosmos-726 R/B	2.3	83.0	1009/963	162	$0.55*10^{-4}$
35	84-72-2	Meteor-2 R/B	2.3	82.5	976/943	185	$0.55*10^{-4}$
36	86-88-1	Polar bear	1.0	89.6	1020/963	177	$0.54*10^{-4}$
37	83-44-17	Cosmos-1461 DEB	4.1	65.0	839/577	151	$0.53*10^{-4}$
38	68-110-2	OAO-2 R/B	11.4	35.0	772/695	127	$0.53*10^{-4}$
39	80-22-2	Cosmos-1168 R/B	2.7	83.0	1009/959	175	$0.52*10^{-4}$
40	79-32-2	Cosmos-1093 R/B	1.9	81.2	598/534	87	$0.52*10^{-4}$
41	73-34-2	Meteor-1 R/B	3.5	81.2	922/857	174	$0.52*10^{-4}$
42	90-5-8	SPOT-2 R/B	3.2	98.5	806/786	207	$0.52*10^{-4}$
43	77-57-2	Meteor-2 R/B	2.0	97.9	620/577	87	$0.52*10^{-4}$
44	71-120-2	Meteor-1 R/B	3.1	81.3	928/863	159	$0.50*10^{-4}$
45	81-84-2	Cosmos-1302 R/B	2.6	74.0	811/770	169	$0.49*10^{-4}$
46	86-18-2	Cosmos-1733 R/B	2.5	82.5	659/624	118	$0.49*10^{-4}$
47	81-117-1	Cosmos-1328	3.5	82.5	646/602	90	$0.48*10^{-4}$
48	82-24-1	Cosmos-1344	1.4	82.9	1033/970	209	$0.47*10^{-4}$
49	84-62-2	Cosmos-1574 R/B	2.6	83.0	1008/965	218	$0.47*10^{-4}$
50	87-87-2	Cosmos-1891 R/B	2.8	82.9	1036/963	168	$0.47*10^{-4}$